



**Universidad**  
Zaragoza



## **Master thesis report**

# **Light-Responsive Nanoparticles as a Novel Draw Solute Materials for Forward Osmosis Desalination Process**

### **Author**

Tarik Hishe Weldeabezgi

### **Supervisors**

Prof. Ivo Vankelecom

Dr. Yusak Hartanto

KU Leuven, Belgium

August 28/2019

# Acknowledgements

I would like to express my deep gratitude to my promotor Professor Ivo VANKELECOM for offering me such a wonderful opportunity to undertake my master thesis work in his group at KU Leuven. His constructive comments and recommendations was truly beneficial. Besides, his door office was always open whenever I ran into a trouble spot or had a question about my research.

I would like also to express my indebtedness appreciation to my daily supervisor Dr. Yusak Hartanto who helped me to improve the experimental designs, lab work, analyses, and writing. His guidance helped me in all the time of research and writing of this thesis. I could not have imagined having a better supervisor for my master thesis work.

I must thank the EM3E-4SW master program for the financial support and giving Erasmus mundus scholarship award to me. In addition, I cannot express enough thanks to all my professors who thought me under this program. My special thanks goes to Prof. Andre Ayrat Prof. Reyes Mallada, and Karin Karlzen for their astonishing support and guidance through the master program.

Last but not the least important, I owe more than thanks to my family members, friends, classmates for their encouragements and support specially during my hardship times.

# Abstract

Clean water shortage is one of the global major concerns. To overcome this problem, membrane-based desalination process, such as reverse osmosis (RO) have been developed in the recent years. However, this technology operates at a high hydraulic pressure to overcome the seawater osmotic pressure, making this desalination process still relatively expensive. Recently, forward osmosis (FO) process has become increasingly attractive over RO since it is capable to produce clean water by using natural osmotic pressure as the separation driving force provided by draw solution (DS), which eliminates the usage of high hydraulic pressure. DS is a critical material in the FO process, playing a key role in determining the separation performance and energy cost. After the FO process, DS requires a regeneration step to reconcentrate it to its initial state. As a result, the development of effective draw solution is essential for the advancement of FO technology.

In this master thesis work, the feasibility of light-responsive TiO<sub>2</sub> nanoparticles was investigated as a draw solute in the FO process. Several dispersions of TiO<sub>2</sub> nanoparticles in demineralized water (DI) with different concentration were prepared. These dispersions were tested for their FO performance with DI and saline water as feed solutions, respectively. The colloidal stability of TiO<sub>2</sub> nanoparticles was achieved by deviation from the isoelectric point of the nanoparticles with a pH adjustment from 6 to 4.5.

The effects of TiO<sub>2</sub> nanoparticle concentration, ultrasonication time, UV irradiation, primary particle size, and FO membrane orientation were tested using DI water as the feed solution. A concentration of 20 g / L of TiO<sub>2</sub> was found as the optimum concentration for FO performance. The generated water flux was not linearly dependent on the nanoparticles concentrations but appeared to be dependent on how well the nanoparticles were dispersed. The effect of UV was investigated by testing the same amount of TiO<sub>2</sub> with and without a UV treatment. The UV treated and sonicated before and after UV treatment generated a significantly higher water flux than the pristine one. The effect of the primary size of the nanoparticles was expressed in their response to UV radiation. In comparison to P5 (=5 nm), P15 (=15 nm), and P25 (= 25 nm), P5 showed the highest UV response. The effect of membrane orientation, namely pressure retarded osmosis (PRO) and forward osmosis (FO) mode were tested and the PRO mode resulted in a significantly

higher water flux than FO mode due to its low concentration polarization effect, which consequently led to higher driving force than FO mode.

The TiO<sub>2</sub> nanoparticles draw solutions were also characterized using DLS and FTIR to investigate the effect of UV on the particle size and hydrophilicity respectively. The DLS result showed a larger hydrodynamic diameter after UV treatment comparing to the pristine one but after ultrasonication, the hydrodynamic diameter was significantly decreased. This result confirmed that UV treatment promoted the agglomeration of nanoparticles. Longer UV irradiation time led to a moderately more hydrophilic surface than the shorter period as confirmed from the FTIR result.

The highest water flux generated with DI water feed solution by using the optimum concentration and parameters without any functionalization or capping agent was 15.8 LMH and this is quite promising.

# Resumen

La escasez de agua limpia es una de las mayores preocupaciones a nivel mundial. Para superar este problema, en los últimos años se han desarrollado varios procesos de desalinización basados en membranas, tales como la ósmosis inversa (OI). Sin embargo, esta tecnología requiere de una alta presión hidráulica para superar la presión osmótica del agua de mar, haciendo que el proceso de desalinización sea relativamente costoso. Recientemente, el proceso de ósmosis directa (OF) se ha vuelto cada vez más atractivo, ya que, a diferencia de la ósmosis inversa (OI), puede producir agua limpia mediante el uso de una solución de alta presión osmótica (DS, por sus siglas en inglés “*draw solution*”), sin necesidad de aplicar altas presiones. El agente osmótico DS es un componente clave en la ósmosis directa, ya que determina el rendimiento de separación y el consumo energía del proceso. Debido a que esta solución requiere un paso de regeneración para reconcentrarla a su estado inicial después del proceso de desalinización, el desarrollo de una solución DS efectiva es esencial para el avance de la tecnología de ósmosis directa.

En este trabajo de fin de máster, se investigó la viabilidad del uso de nanopartículas de  $\text{TiO}_2$  sensibles a la luz como un agente osmótico DS para el proceso de ósmosis directa. Para esto, se prepararon dispersiones de diferente concentración de nanopartículas de  $\text{TiO}_2$  en agua desmineralizada (DI). Estas dispersiones se probaron para su rendimiento en ósmosis directa con DI y agua salina como soluciones de alimentación, respectivamente. La estabilidad coloidal de las nanopartículas de  $\text{TiO}_2$  se logró por desviación del punto isoelectrico de las nanopartículas ajustando el pH de 6.0 a 4.5.

Los efectos de la concentración de nanopartículas de  $\text{TiO}_2$ , el tiempo de ultrasonidos, la irradiación UV, el tamaño de partícula primaria y la orientación de la membrana OD se probaron usando agua DI como solución de alimentación. Se encontró que una concentración de 20 g/L de  $\text{TiO}_2$  era la concentración óptima para el rendimiento OD. El flujo de agua generado no dependió linealmente de la concentración de nanopartículas, pero pareció depender de qué tan bien era su dispersión. El efecto de los rayos UV se investigó probando la misma cantidad de  $\text{TiO}_2$  con y sin tratamiento con rayos UV. El tratamiento con UV y la sonicación antes y después del tratamiento con UV generó un flujo de agua significativamente mayor que el original. El efecto del tamaño primario de las nanopartículas se expresó en su respuesta a la radiación UV. En comparación con P5 (= 5 nm),

P15 (= 15 nm) y P25 (= 25 nm), P5 mostró la respuesta UV más alta. Se probó el efecto de la orientación de la membrana, tanto en el modo de ósmosis retardada por presión (PRO) y de ósmosis directa (OD). El modo PRO exhibió un flujo de agua significativamente mayor que el modo OD debido a su efecto de polarización de baja concentración, produciendo, como consecuencia, a una mayor fuerza de conducción que el modo OD.

Las soluciones DS de nanopartículas de TiO<sub>2</sub> también se caracterizaron utilizando DLS y FTIR para investigar el efecto de los rayos UV sobre el tamaño de partícula y la hidrofiliidad, respectivamente. El resultado de DLS mostró un diámetro hidrodinámico mayor después del tratamiento con UV en comparación con el prístino, pero después de la sonicación con ultasonidos, el diámetro hidrodinámico disminuyó significativamente. Este resultado confirmó que el tratamiento con UV promovió la aglomeración de nanopartículas. Un tiempo de irradiación UV más prolongado condujo a una superficie moderadamente más hidrofílica que el período más corto, según lo confirmado por el resultado de FTIR.

El flujo de agua más alto generado con la solución de alimentación de agua DI, utilizando la concentración y los parámetros óptimos sin ningún agente de funcionalización o de cobertura, fue de 15.8 LMH lo cual es bastante prometedor.

## Table of Contents

<b>Acknowledgements</b> .....	i
<b>Abstract</b> .....	ii
<b>Resumen</b> .....	iv
<b>List of Figures</b> .....	vii
<b>1. Introduction</b> .....	2
<b>1.1 Objective</b> .....	6
<b>2. Literature review</b> .....	6
<b>2.1 Concentration polarization and FO operational modes</b> .....	9
<b>2.2 Potential of titanium dioxide nanoparticles as draw agent</b> .....	10
<b>3. Experimental part</b> .....	12
<b>3.1 Materials</b> .....	12
<b>3.3 Characterization</b> .....	13
3.3.1 FO experiment .....	13
3.3.2 Dynamic light scattering (DLS) .....	14
3.3.3 FO-Desalination.....	15
<b>4. Result and discussion</b> .....	15
<b>4.1. FO experiment</b> .....	15
4.1.1. Effect of UV and content of TiO <sub>2</sub> on water flux .....	15
4.1.2 Effect of ultra-sonication .....	18
4.1.3 Effect of concentration of TiO <sub>2</sub> nanoparticle.....	20
4.1.4. Effect of particle size of TiO <sub>2</sub> .....	22
4.1.5 Effect of membrane orientation .....	23
<b>4.2 Dynamic light scattering (DLS)</b> .....	25
<b>4.3 FTIR</b> .....	26

4.4 Recovery method .....	27
5 Conclusion .....	28
References .....	29

## List of Figures

<b>Fig.1.</b> Representation of an FO process with pre-treatment and post-treatment .....	8
<b>Fig. 2</b> Illustrations of concentration polarization in FO: (a) PRO-mode (b) FO-mode orientation (RE-printed from reference [30]).....	10
<b>Fig. 3</b> Superamphiphilicity of TiO <sub>2</sub> : (a) (Before UV illumination) the OH group is bound to oxygen vacancy, (a) (at the transition state) the photoexcited hole is trapped at the lattice oxygen, and (c) (after UV irradiation) new OH groups are formed [48].....	11
<b>Fig. 4.</b> Draw solution preparation process and the FO laboratory set up .....	13
<b>Fig.5.</b> Schematic set-up of the FO laboratory experiment.....	14
<b>Fig. 6.</b> Effect concentration of TiO <sub>2</sub> on water flux in FO experiment.....	15
<b>Fig. 7.</b> Reproducibility result: Effect of concentration of TiO <sub>2</sub> on water flux in FO experiment	16
<b>Fig. 8.</b> Effect of ultrasonication on the performance of the draw solution using: (a) 2g/L, and (c) 5 g/L of of TiO <sub>2</sub> nanoparticle ultrasonicated for 25 min without UV treatment, (b) 2 g/L, and (d) 5 g/L of TiO <sub>2</sub> nanoparticle ultrasonicated for 25 min before 1 h UV treatment. All draw solutions were adjusted to a pH of 4.5. ....	17
<b>Fig. 9.</b> Reproducibility result: Effect of ultrasonication on the performance of the draw solution .....	18
<b>Fig. 10.</b> Effect of sonication of the draw solution before and after UV treatment ( a) sonicated before UV (b) sonicated before and after UV for 25 min: 5g/L TiO <sub>2</sub> NPs at pH = 4.5.....	19
<b>Fig.11.</b> Reproducibility result: Effect of sonication of the draw solution before and after UV treatment .....	19
<b>Fig.12.</b> Effect of sonication time after 1 h UV treatment of the draw solution on the water flux in FO using 5g/L TiO <sub>2</sub> NPs sonicated for 25 min before 1 h UV treatment.....	20
<b>Fig. 13.</b> Effect of concertation of TiO <sub>2</sub> on water flux: sonicated for 25miun before and after 1 h UV irradiation at pH = 4.5.....	21

<b>Fig. 14.</b> Reproducibility result of 20 g/L .....	21
<b>Fig.15.</b> Effect of particle size of TiO <sub>2</sub> in draw solution performance in FO water flux: (a) P5, (b) P15, (c) P25 nm size. ....	22
<b>Fig.16.</b> Reproducibility result: Effect of particle size of TiO <sub>2</sub> in draw solution performance in FO water flux .....	23
<b>Fig. 17.</b> Effect of membrane orientations on the FO water flux. (a) PRO mode, (b) FO mode ...	23
<b>Fig. 18.</b> Feed solution weight versus time profile recorded using 20 g/L TiO <sub>2</sub> draw solution without UV treatment sonicated for 25 minutes before FO experiment with 500 ppm NaCl feed solution. ....	24
<b>Fig. 19.</b> Weight change of the feed solutions and evaluated Water fluxes based on the weight change of the feed solutions in 2h FO process by employing 20 g/L of TiO <sub>2</sub> concentration ultrasonicated for 25 minutes before and after UV treatment as draw solution. Weight change measured: (a) 500 ppm and (b) 1000 ppm NaCl solution feed solutions. Water fluxes calculated by using: (C) 500 ppm, and (d) 1000 ppm NaCl solutions as a feed solution. ....	25
<b>Fig.20.</b> FO desalination with 20 g/L TiO <sub>2</sub> draw solution and 100 ppm NaCl feed solution: (a) weight versus time change of the feed solution, (b) water fluxes evaluated based on the weight change of the feed solution in time. ....	25
<b>Fig. 21.</b> Effect of UV treatment on the hydrodynamic diameter of the nanoparticles (in log to base 10): (a) = P5, (b) = P15, (c) = P25 .....	26
<b>Fig. 22.</b> FTIR result shows the effect of UV irradiation time on the chemical composition of TiO <sub>2</sub> NPs .....	27
<b>Fig.23.</b> TiO <sub>2</sub> regeneration process from the diluted TiO <sub>2</sub> draw solution via two main consecutive processes: (1) dark storage, and (2) low-pressure Ultrafiltration processes .....	27



The EM3E4SW Master is an Education Programme supported by the European Commission, the European Membrane Society (EMS), the European Membrane House (EMH), and a large international network of industrial companies, research centres and universities" ([www.em3e.eu](http://www.em3e.eu)).

The EM3E4SW education programme has been funded with support from the European Commission. This publication reflects the views only of the author, and the Commission cannot be held responsible for any use which may be made of the information contained therein".

El Máster EM3E4SW es un programa educativo apoyado por la Comisión Europea, la Sociedad Europea de Membranas (EMS), la Casa Europea de Membranas (EMH) y una gran red internacional de empresas industriales, centros de investigación y universidades " ([www.em3e.eu](http://www.em3e.eu)).

El programa educativo EM3E4SW ha sido financiado con el apoyo de la Comisión Europea. Esta publicación refleja solo las opiniones del autor, y la Comisión no se hace responsable del uso que pueda hacerse de la información contenida en el mismo".

# 1. Introduction

Freshwater scarcity has become one of the most contemporary challenges of the world, caused by different factors including fast population growth, intensive urbanization and industrialization, and climate change[1]. A recent report disclosed that more than 1.2 billion people lack access to clean potable water [2]. Around 71% of the earth surface is enclosed with water, however, less than 1% is the freshwater. The rest of the water is either very saline or not accessible. Researchers have attempted to develop an engineering solution to alleviate water scarcity using desalination process. Desalination is a process to remove salts from water aquifers such as ocean/seawater, brackish and produced water.

Desalination has been regarded as a promising technology to mitigate the shortage of potable water. In general, desalination can be classified into two main groups: membrane and thermal process. The thermal process is one of the oldest desalination technology that has been used for many years, and considerably resolved the shortage of water. In this process, thermally energy is employed to vaporize the water feed solution and then the vaporized water is condensed and collected to obtain clean water. In the membrane process, a semipermeable membrane, which is act as a selective barrier, is used to remove salt from seawater. Thermal-based desalination process includes multiple effect distillation (MED) and multistage flash distillation (MSF) and membrane-based desalination includes reverse osmosis (RO), electrodialysis (ED), forward osmosis (FO), membrane distillation (MD) and pervaporation (PV). The general classification of desalination technology is presented in Fig.1. For several years, the thermal process was the predominant desalination technology, where are presently, membrane process is becoming the main means of desalination technique due to the extraordinary advancement of membrane technology, owing to high separation efficiency, pleasing operational cost, low chemical and energy consumption compared to thermal process[3], [4].[5].

Of all the existed desalination technology, MED, MSF and RO take the highest market share accounting around 93% of the total worldwide desalination installed plants. The MSF process is one of the earliest methods of water purification, established technology appropriate for industrial desalination application, however, it's high energy demand and low heat transfer efficiency call forth for other alternatives [6]. Currently, RO is the most mature and leading desalination

technology with a share of around 74%, while MED and MSF account 8% and 11% respectively, of the 93%[7]. RO overtakes thermal processes in the new installation of the plant since RO consumes less energy and small footprint compared to thermal process [8] .

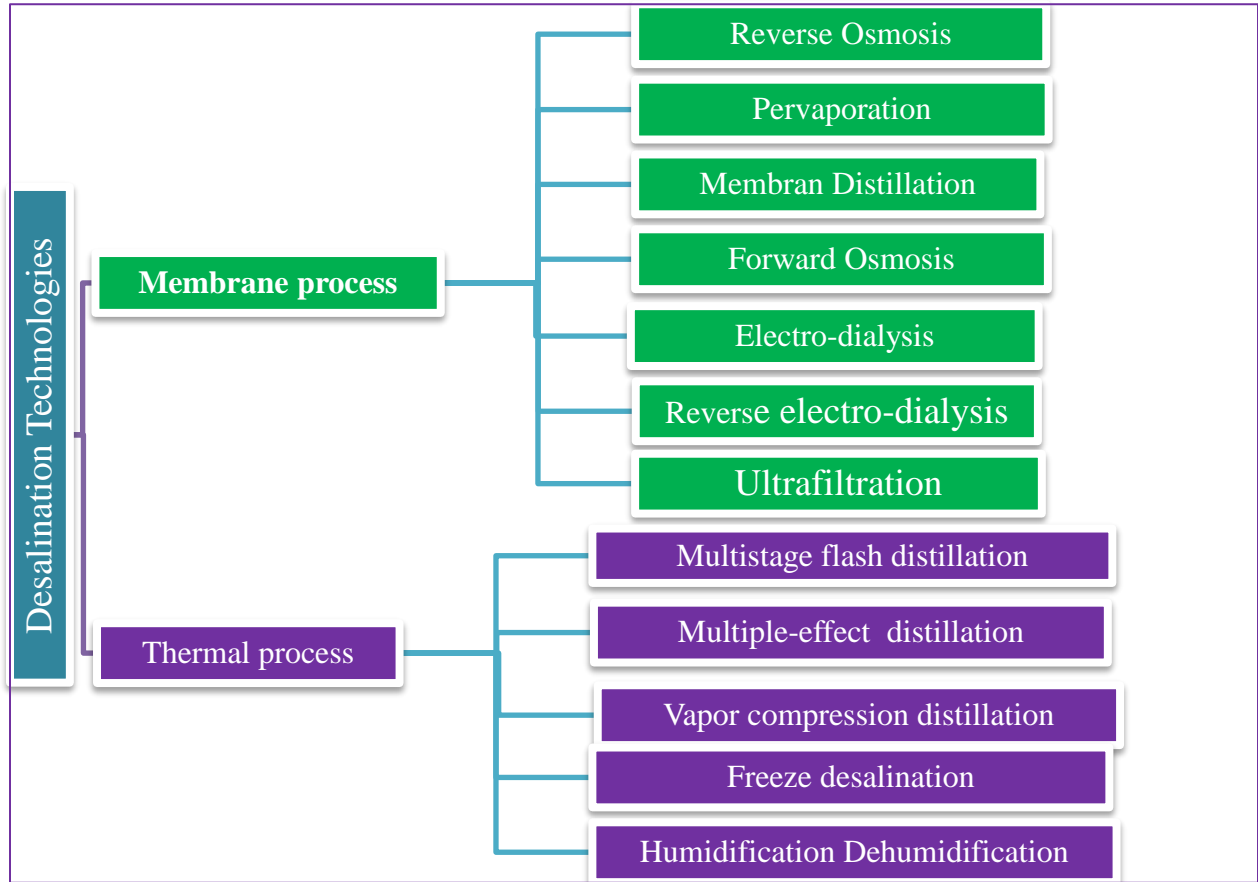


**Fig. 1.** The general classification of water desalination technologies

In general, numerous factors should be considering for economic analysis of desalination technologies. Among the factors are feed water quality, plant capital cost, energy cost and waste management and others. Among all those aforementioned factors, energy accounts the largest portion of cost in all desalination system [9]. A substantial extent of the shift toward membrane-based desalination has been inspired due its lower energy consumption. The energy requirement for the commonly used technologies for desalination is provided in table-1. In this report, I made discrepancy between thermal and electrical energy.

**Table.1.** Comparison of specific energy consumption of the common methods of desalination technologies[10]–[14].

Membrane type	Specific energy consumption(kWh/m <sup>3</sup> )		
	Electrical	Thermal	Total electric equivalent
SWRO	3-6	-	3-6
ED	1-3.5	-	1-3.5
EDR	1-2	-	1-2
FO	20-150	-	10-68
MD	1.5-4	4-40	3-22
MSF	2.5-5	40-120	21-59
MED	2-2.5	30-120	15-57
MVC	7-15	-	7-15

SWRO= seawater reverse osmosis, ED=Electro dialysis, EDR= electro dialysis reversal, FO=forward osmosis, MD=Membrane distillation, MSF=Multi stage effect, MED= multi effect distillation, MVC=Mechanical vapor compression,

There are around 15,000 desalination plants installed and under operation through the world and approximately 69% of the total desalination plants are covered by RO plants[15].

In RO membrane process, high pressure is applied to the feed solution to overcome the intrinsic osmotic pressure so that water can be transported through the membrane. However, if the feed solution contains high total dissolved solute (TDS) concentrations, RO requires a huge hydraulic pressure to overcome the osmotic pressure of the feed solution and this is one of the most challenging issues in RO-based desalination. Moreover, to protect the membrane from fouling, usually, RO requires an extensive pre-treatment of the feed solution before contacting the membrane. Therefore, membrane fouling could be also another impediment. The efficiency of RO water recovery spans from 35% to 85% and also, and the retentate stream which have high salt concentration is a problem that can cause secondary pollution and hence needs appropriate brine management system.[5][16].

Forward osmosis (FO) has been considered as a promising alternative membrane technology for water reuse and desalination because its advantages over classical desalination technologies. In FO, the main driving force is the osmotic pressure difference between two solutions separated by a semipermeable membrane. FO utilizes less energy comparing with other desalination

processes such as RO and distillation since it is operated under osmotic pressure gradient induced by concentrated draw solutes without providing other external forces such as electrical or mechanical energy. Furthermore, FO exhibits less fouling tendency compared to other pressure driven membrane process [4][17][18].

Even though FO has been known as a promising and energy-efficient desalination technology there are technical problems related to applying FO in large scale process. The draw solution is the main component of the FO that controls the overall performance since it has to generate enough osmotic pressure to accomplish high water flux. Moreover, the transferred water through the semi-permeable membrane has to be separated easily from the draw solution. The suitable draw solution must be non-toxic, economical, and able to be regenerated after a long term usage without losing its performance. Regenerating of draw solution requires considerable energy which made FO be difficult for large scale application. Thus, it is necessary the draw solution to be recovered as simple as possible [19], [20].

To develop an energy-efficient FO desalination system, a suitable membrane and draw solution must be accurately designed and carefully chosen. In the last few decades, different draw solutions have been discovered including inorganic salts such as  $MgCl_2$ ,  $MgSO_4$ ,  $NaCl$ , and organic salts like 2-methylimidazole, thermolytic agents such as ammonium bicarbonate ( $NH_4HCO_3$ ) [17], [21], [22] and stimuli-responsive materials [20], [23]. However, there is no report on the draw agent that satisfy the ideal criteria parameters of draw agent for FO such as attractive osmolality to generate high osmotic pressure and easily regeneration from water.

In this master thesis work,  $TiO_2$  nanoparticles which are categorized as light-responsive draw solution is proposed as a draw solute to extract water from DI water and saline feed stream across a semi-permeable membrane. Laboratory scale-experiments with a semi-permeable thin-film composite (TFC) was used to investigate the feasibility of the  $TiO_2$  nanoparticles in FO experiment as a draw solution. The draw solution was characterized using different techniques such as water flux in FO, DLS, and FTIR.

## 1.1 Objective

The main objectives of this master thesis work were;

- ❖ To investigate the feasibility of light-responsive pristine inorganic nanoparticle ( $\text{TiO}_2$ ) as to draw agent for forward osmosis (FO) desalination.
- ❖ To modify  $\text{TiO}_2$  draw agent using different parameters (e.g. pH adjustment, size, UV treatment) and examine its effect in FO water flux.
- ❖ To investigate the effect of membrane orientation and nanoparticle primary size in FO water flux
- ❖ To characterize the prepared draw agent using DLS and FTIR.

## 2. Literature review

Since 98% of the world's accessible water supply is sea or brackish water, desalination of these resources is becoming progressively key means to mitigate the shortage of freshwater resources especially in regions with extreme water resources like North Africa, Middle East, eastern Australia, parts of Central and South Asia, and the southwestern areas of North America [24]–[26]. Stem from different parameter such as feed and permeate water quality, energy utilization and desired capacity various membrane and thermal-based desalination techniques have been employed to desalinate saline water. At this time, reverse osmosis (RO) and multi-stage flash (MSF) are the most widely implemented methods. For countless scientists around the planet, the evolution of a new desalination technique with less energy requirement, infrastructure costs, and carbon footprint has been a hot research issue.

Forward osmosis is an emerging membrane technology used for desalination, which has a capacity to alleviate the problems related to high energy utilization of other desalination techniques. FO needs considerable innovation to develop a draw solution that can achieve a acceptable water flux and less energy consumption to recover the draw agent. Researchers have developed different types of draw solution and conducted their performance in FO for desalination. However, due to the difficult of draw agent recovery and also low water flux, FO is lagging from commercialization. Therefore, discovering a suitable draw solute material plays a major role in developing a promising FO process.

Forward osmosis (FO) is an evolving process which is driven by an osmotic pressure gradient comprising a semipermeable membrane and a draw solution. Theoretically, the semipermeable membrane acts as a barrier that rejects salts or undesirable components, but permits water to pass through, while the draw solution (high osmotic pressure) withdraws water across the semipermeable membrane from the feed solution (low osmotic pressure) side [27], [28]. Since FO functions at low pressures and low temperatures dissimilar to pressure-driven membrane processes (such as RO) it provides numerous possible benefits like less energy input and membrane fouling. As FO utilizes a concentrated draw solution to produce osmotic pressure, which attracts water across a semi-permeable membrane from the feed solution, the feed stream decreases in volume, raising the salt concentration, which leads to low permeate flux to the draw solution side [18], [29]. FO processes follow the second law of thermodynamics where solvent molecules transport spontaneously from a low concentration solution through a semipermeable membrane to a high concentration solution so as to counterbalance their overall chemical potential [30], [31]. The general equation for calculation of water flux of the osmotic processes is given as:

$$J_W = A(\sigma\Delta\pi - \Delta P) \quad (1)$$

Where  $J_W$  is the water flux,  $A$  the water permeability constant of the membrane,  $\sigma$  the reflection coefficient, and  $\Delta P$  is the applied pressure. For FO,  $\Delta P$  is zero; for RO,  $\Delta P > \Delta\pi$ .

In FO desalination, after the withdrawal of water from the feed, a second step (dewatering) is often required for the production of freshwater and regeneration of the draw solute [32]. This is the only step that needs energy input, so a suitable draw solute is needed to increase the efficiency and sustainability of FO operations. A particular FO desalination process is displayed in Fig. 1.

For developing the FO process, the selection of appropriate draw solutes is indispensable. A correct draw solution helps to advance the effectiveness of the FO process and also to keep the expenses of the successive stages (retrieving and replacing the draw solute) [30]. Besides, the draw solute should possess low cost and toxicity, small molecular weight and low in its aqueous solution and in general, an ideal draw solution should satisfy the following criteria: high osmotic pressure, low reverse flux, and easy regeneration mechanism.

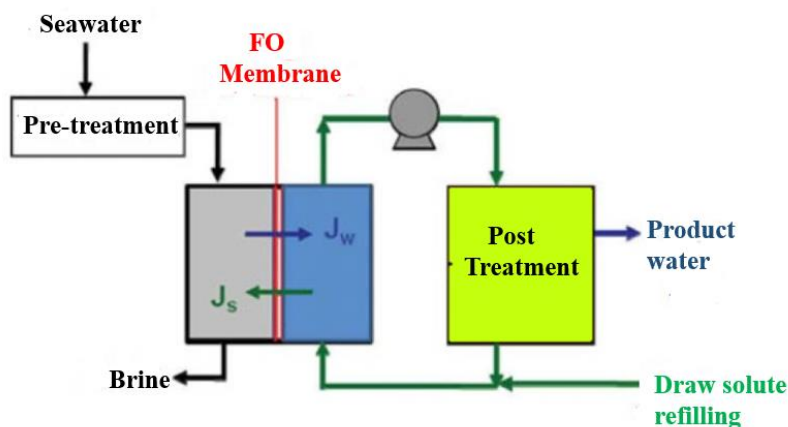


**Fig.1.** Representation of an FO process with pre-treatment and post-treatment

Numerous types of draw agents for FO desalination have been reported in the literature. For example, Sun et al[33] reported for the first time the suitability of magnetic nanoparticle to be used for FO as smart draw solution. The prepared MNPs were tested in the FO system for desalting of brackish water. It was demonstrated that those MNPs are competent in drawing clean water from brackish which produce high osmotic pressure. Besides, Amy et al[34] reported magnetic nanoparticles (MNPs) as novel draw solutes in the FO process. This discovery mitigated the problem associated with salt leakage, however, during recovering/regeneration of the nanoparticle agglomeration was observed which limits them to be used for large scale application. Besides, water flux is low. Furthermore, other draw agents such as ethanol[35], thermo-sensitive polyelectrolyte of poly(*N*-isopropyl acrylamide-*co*-acrylic acid) (PNA) [26], polymer-carbon nanotubes composite hydrogel[36] and others have been developed and tested their performance in FO technology. Though some of them showed a good feature of recovery from the diluted draw solution, the water flux achieved is not yet viable for commercialization, the regeneration process of the draw agent consumes a lot of energy and also some of the dewatered water is not safe for human consumption, water separated from volatile draw solutes, since it is difficult to completely eliminate these draw solutes from the pure water. Due to the lack of suitable draw solute, FO technology has been hindered from commercial implementation.

The state of art review on the recent draw solutes are discussed and provided in table-2. Draw solutes can be organic, inorganic and hybrid of both materials.

Nanoparticle were used as novel draw solutes due to their ease recovery and lower energy consumption Table-2 shows the recent draw solutes (DS) with their respective performance.

**Table -2:** State of art on the recent draw solutes used in FO process

Draw agent	Type	Osmotic pressure	Water flux(LMH)	Recovery method	Ref.
PAspNa	Organic	44.5 atm (DS: 0.72 g/mL)	17 (DS: 0.3 g/mL, Feed: Distilled Water)	NF	[37]
Switchable polarity solvents	Volatile Compound	325 atm (DS: 7.6 mol/kg)	18.8 (DS: 7.6 mol/kg, Feed: 0.5 M NaCl)	CO <sub>2</sub> -RO	[38]
Magnetic nanoparticles modified with 2-pyrrolidine, tri-ethylene glycol and PAA	Hybrid	NA	2.4–7.5 LMH (FO mode) and 2.8–10.3 LMH (PRO mode)	Magnetic field	[39]
Pure hydrogels (PSA-MBA, PNIPAM-MBA, PNIPAM-coSA, PAM-MBA)	Organic	50°C and 30 bar (2 min)	0.96 (PSA-MBA)–0.27 LMH (PNIPAM-MBA)	NA	[40]
PSS	Organic	NA	18.2 (DS: 240 g/L, Feed: 0.5 M NaCl)	RO/UF	[41]
PSSS-PNIPAM	Organic	800–2200 mOsmol/kg (DS: 5–15% wt.)	4 (DS: 33.3 wt.%, Feed: 0.6 M NaCl)	MD	[42]
(Triton X-100) to Na <sub>3</sub> PO <sub>4</sub>	Inorganic	38 atm (DS: 0.55 M)	4.9 (DS: 0.55 M, Feed: Brackish water 4090 ppm)	UF/NF	[43]
Cupric and ferric hydroacid complexes	Inorganic	80 atm (DS: 2 M)	17.4 (DS: 2 M, Feed: 3.5%wt. NaCl)	FO/NF	[1]

Poly (sodium styrene-4-sulfonate)-co-poly(N-isopropylacrylamide) = PSSS-PNIPAM

DS = Draw solution

## 2.1 Concentration polarization and FO operational modes

Despite desirable features of FO for desalination, FO desalination operation is significantly hindered by concentration polarization (CP) caused mainly as a consequence of sublayer structure of FO membrane. As a result, the influence of CP need to be taken into consideration.

There are two types of CP for an FO process: internal concentration polarization (ICP) if CP occurs within the membrane sublayer and external concentration polarization (ECP) if CP occurs at the membrane surface. Since the feed is always concentrated and the draw solution is always diluted in the FO process, there exists concentrative CP and dilutive CP at the feed and draw solution sides, correspondingly [30]. In FO mode (when the feed is on the selective layer), there

exists concentrative ECP at the feed side and dilutive ICP at the draw solution side (Fig. 2 right). Likewise, in PRO mode (when the draw solution is facing selective layer), there will be concentrative ICP and dilutive ECP (Fig. 2 left).

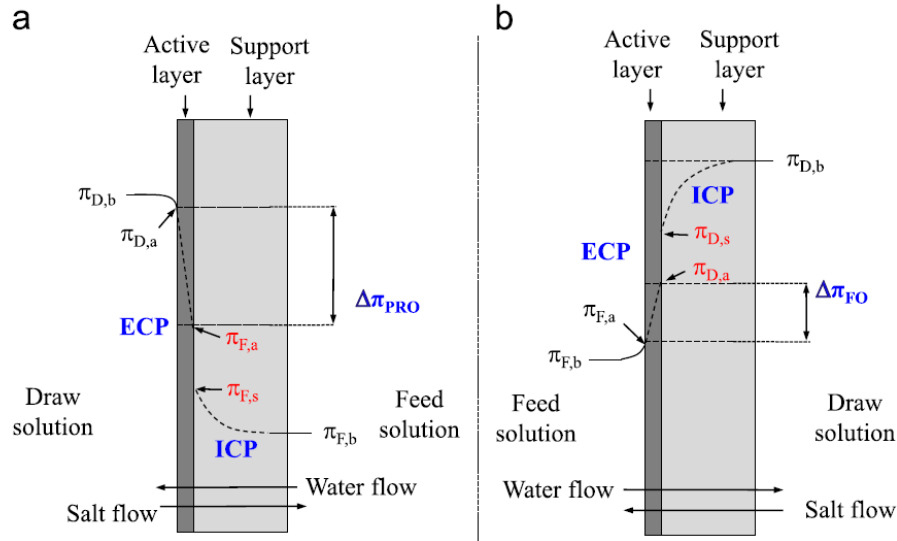


**Fig. 2** Illustrations of concentration polarization in FO: (a) PRO-mode (b) FO-mode orientation (RE-printed from reference [30])

Because of concentration polarization, the effective osmotic pressure across the membranes declines and  $\pi_{D,a} - \pi_{F,a}$  will become lower than  $\pi_{D,b} - \pi_{F,b}$ . In Fig. 2,  $\pi_{D,a}$ ,  $\pi_{F,a}$ ,  $\pi_{D,b}$  and  $\pi_{F,b}$  are the osmotic pressures of the draw solution and the feed at membrane active layer surfaces, and bulky solutions in draw solution and feed solution, respectively [7]. The modified version of equation (1) after considering concentration polarization will be:

$$J = A\sigma\Delta\pi = A\sigma(\pi_{D,a} - \pi_{F,a}) \quad (2)$$

The impact of ICP cannot be effectively minimized since ICP happens and exists within the porous sublayer instead of at membrane surface [21]. However, ECP can be alleviated by increasing the shear rate and turbulence of flow across the membrane [44].

## 2.2 Potential of titanium dioxide nanoparticles as draw agent

Researchers have found that UV illumination of TiO<sub>2</sub> materials can produce a highly amphiphilic surface. This phenomenon is considered to be due to structural changes of TiO<sub>2</sub> itself [45], [46], which proceed completely different from the conventional photocatalytic oxidation reactions. UV-irradiation led to reconstruction of hydroxyl groups (Fig 3a-C). As illustrated in Fig.

3, if the photon has a higher energy than the bandgap ( $\sim 3.2$  eV), electrons are excited from the valence band and holes are formed at the valence band,  $\text{Ti}^{4+}$  gets reduced to  $\text{Ti}^{3+}$ . These photoexcited electrons and holes can recombine or can diffuse through the material. Photoexcited holes reaching the surface results in a new hydroxyl groups at the surface by water adsorption, which makes  $\text{TiO}_2$  hydrophilic [47]. During the dark storage, hydroxyl groups gradually desorbed from the surface in the form of  $\text{H}_2\text{O}_2$  or  $\text{H}_2\text{O} + \text{O}_2$ . This alternation of irradiation and dark storage causes the reversible wettability of  $\text{TiO}_2$  [48].

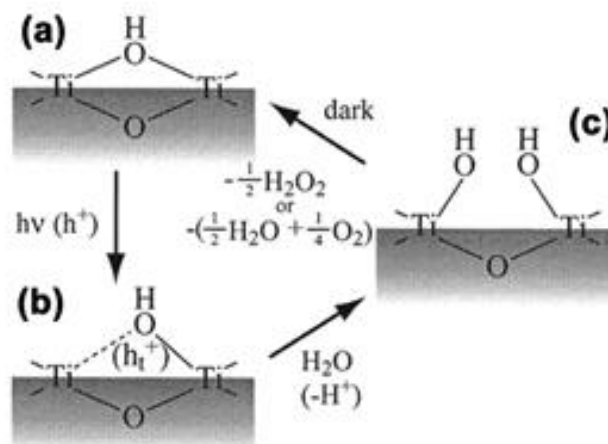


**Fig. 3** Superamphiphilicity of  $\text{TiO}_2$ : (a) (Before UV illumination) the OH group is bound to oxygen vacancy, (a) (at the transition state) the photoexcited hole is trapped at the lattice oxygen, and (c) (after UV irradiation) new OH groups are formed [48].

In this study, inorganic nanoparticles ( $\text{TiO}_2$ ) were studied as a drawing agent for FO desalination owing to their stimuli-responsive properties and ease of recovery. The drawing capability of  $\text{TiO}_2$  nanoparticles was investigated using both DI and brackish water as feed solution.  $\text{TiO}_2$  nanoparticles were chosen in this study due to their easy recovery of the diluted draw solution, cheap and possesses less toxicity. The result demonstrated that  $\text{TiO}_2$  nanoparticle can draw DI water with attractive water flux –reaching  $>14$  LMH and also, it was observed that they can be used for desalination of brackish water with low feed salt concentration. Moreover,  $\text{TiO}_2$  nanoparticle can be easily regenerated from the diluted draw solution by storing the diluted solution in dark environment, in which the nanoparticles are sediment and the water is filtered, and then the water could be further purified using ultrafiltration membrane.

## 3. Experimental part

### 3.1 Materials

Titanium dioxide nanoparticles (TiO<sub>2</sub> P25 AEROXIDE weight ratio anatase/rutile = 80/20) supplied from Evonik Industries was used as a draw solution. Commercial thin-film composite (TFC) FO membrane was provided by Hydration Technology Innovations (HTI, OR, USA). Sodium chloride with analytical reagent grade (NaCl, ≥99.5%). Ultrapure water was supplied by a MilliQ ultrapure water system (Millipore, Bedford, MA, USA). HCl (37 %, Fisher Scientific) used as stabilization agent. All chemicals were used as received without purification.

### 3.2 Draw solution preparation

The draw solution was prepared using the following protocol. Different content of TiO<sub>2</sub> nanoparticles was dispersed in 100 mL of DI water and stirred overnight. After a day, the homogenous draw solution was sonicated by ultra-sonicator (Branson Digital Sonifier (Branson Ultrasonics Corporation, USA) at 40% amplitude and at different period of time depending on the amount of TiO<sub>2</sub>, to prevent aggregation and disperse the nanoparticles. Then, ultraviolet treatment takes place, where the TiO<sub>2</sub> solution was placed in a UV oven (LZCICH2 photoreactor, Luzchem) for a different period of time while stirring was kept. LZC-UVA lamps – fluorescent lamps (8 Watt) which comprises the 320 – 400 nm range were used. The UV treatment was intended to enhance the hydrophilicity of the nanoparticles. To observe the effect of UV on driving force, the draw solutions were tested in FO experiment with and without treatment of the UV.

The summary of the draw solution preparation process and the FO laboratory set up is provided in Fig.4.

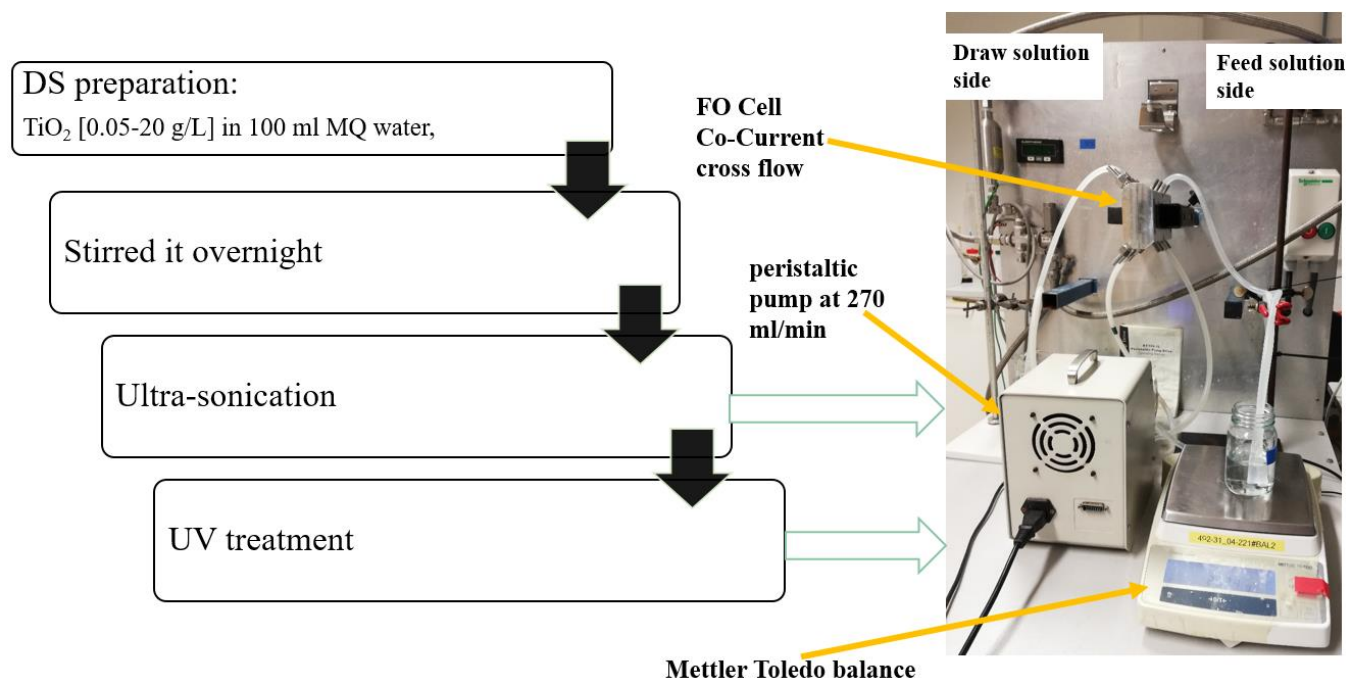


**Fig. 4.** Draw solution preparation process and the FO laboratory set up

### 3.3 Characterization

#### 3.3.1 FO experiment

The performance of the prepared draw agent was evaluated in FO laboratory experiment. Fig.5 shows the laboratory scale apparatus of the FO set-up. The different draw solutions were placed in a custom-made high throughput lab-scale crossflow FO cell with 2 channels, enabling 4 different variations in feed/draw/membrane condition per run. In this experiment, one of the channels was used. The cell comprised of a rectangular channel with a 55 mm length, a 15 mm width and a 2 mm depth with an active membrane surface of 8.25 cm<sup>2</sup> was used. The commercial HTI-TFC membrane in PRO mode (Active layer faced to the draw solution) was tested as the default membrane configuration first with DI Water at different concentration of TiO<sub>2</sub> nanoparticles to select the optimum concentration that yields higher water flux. Then, the performance of the draw solution was also performed using different feed salt concentration.

Both the draw and feed solutions (100 mL and 150 ml respectively) were circulated under a co-current flow by a peristaltic pump at 270 mL/min with a spacer while stirring the draw solutions (500 rpm).

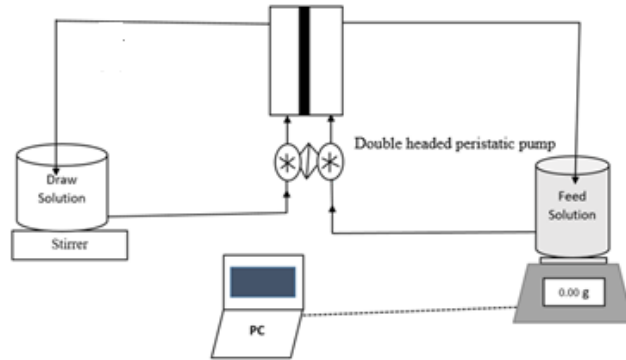


**Fig.5.** Schematic set-up of the FO laboratory experiment

The water flux was measured by recording the mass of the stirred draw solution on a balance (PB8001-S/Fact, Mettler Toledo). The water flux was in terms of (Liter per Meter square per Hour, (LMH)) was calculated according to Equation 1.

$$J_w = \frac{\Delta m}{A \cdot \rho \cdot \Delta t} \quad (1)$$

Where,  $J_w$  water flux (LMH),  $\Delta m$  change of mass (g),  $A$  is the effective area of the membrane ( $m^2$ ) and  $\rho$  is the density of the feed solution (g/L).

### 3.3.2 Dynamic light scattering (DLS)

The hydrodynamic diameter of the  $TiO_2$  dispersions was determined using particle size analyzer (Nano Plus 3, Particulate Systems, Micromeritics Instrument Corp.). It gives the particle size distribution in the solution. The hydrodynamic diameter of draw solutions: 1) without UV treatment, 2) with UV treatment, 3) With ultrasonication after UV treatment were measured. The measurement was carried out at room temperature.

### 3.3.3 Fourier-transform infrared spectroscopy

The chemical composition and hydrophilicity switch of the draw solution at different UV irradiation time was determined using Fourier-transform infrared spectroscopy (FTIR) (Alpha, Bruker, USA).

### 3.3.3 FO-Desalination

After discovering the optimum concentration of TiO<sub>2</sub> NPs that results in higher water flux with DI water feed solution; its feasibility as a draw solution in FO-Desalination experiment was also investigated with saline water feed solutions containing NaCl concentration ranging from 100ppm-1000ppm in PRO mode. Water flux evaluation was conducted for three types of draw solutions: 1) Pristine, 2) UV treated and 3) Citric acid-modified TiO<sub>2</sub> NPs.

## 4. Result and discussion

### 4.1. FO experiment

#### 4.1.1. Effect of UV and content of TiO<sub>2</sub> on water flux

The draw solution was evaluated its osmotic pressure in terms of water flux. TiO<sub>2</sub> nanoparticles (NPs) are stimuli-responsive materials that can shift their hydrophilicity by exposing to UV irradiation. The performance of draw solution consisting of TiO<sub>2</sub> nanoparticle was evaluated by varying the period of sonication and UV irradiation. Fig. 6.shows the effect of TiO<sub>2</sub> nanoparticle content on the water flux in FO experiment.

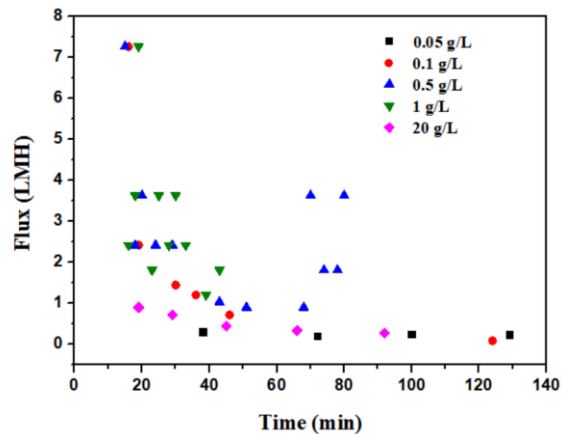


**Fig. 6.** Effect concentration of TiO<sub>2</sub> on water flux in FO experiment

The experimental result shown in Fig. 6 was repeated two times to check its reproducibility and the result are shown in Fig.7.

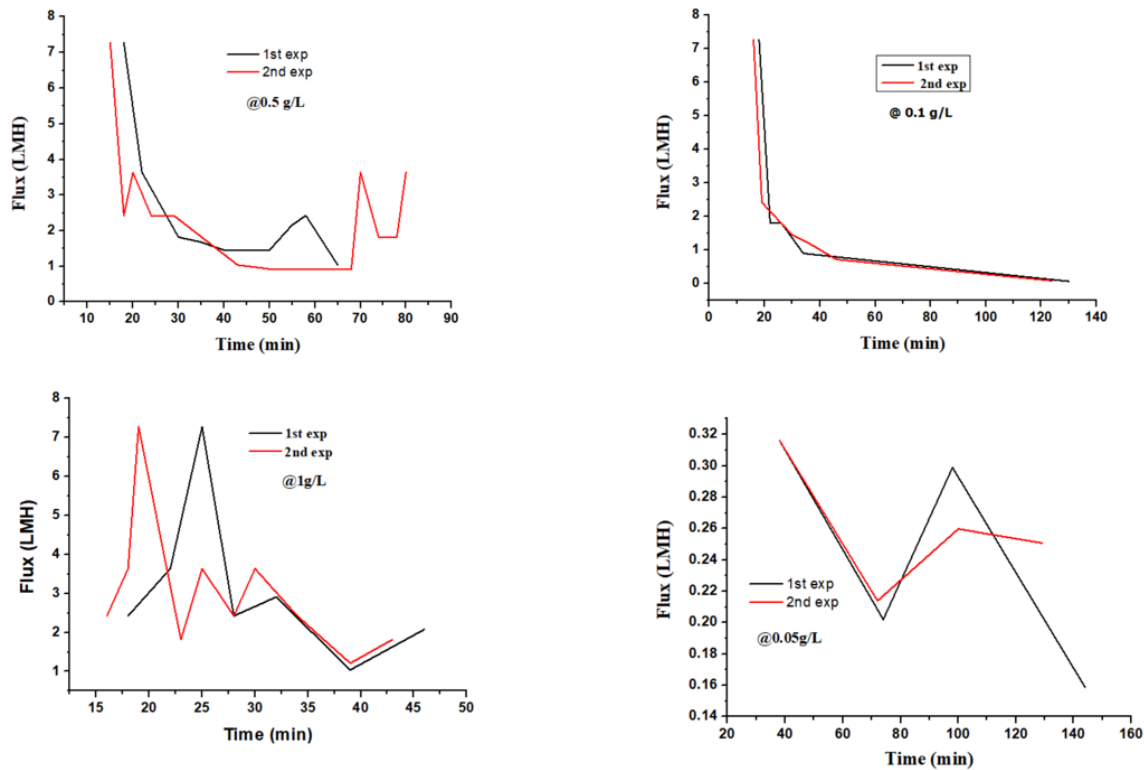


**Fig. 7.** Reproducibility result: Effect of concentration of TiO<sub>2</sub> on water flux in FO experiment

In this experiment, DI water was used as a feed solution and the draw solution was prepared by mixing of the different content of TiO<sub>2</sub> NPs in DI water. Before UV treatment, all the draw solutions were sonicated for 10 min and then, irradiated for 1 h in UV. It can be seen from the Fig.6 that different content of TiO<sub>2</sub> NPs in the draw solution exhibited a significant difference in attracting water. For example, at 0.1, 0.5 and 1g/L of TiO<sub>2</sub> showed a higher water flux while lower or higher than of this concentration revealed a lower water flux. This suggests that an optimum content of TiO<sub>2</sub> should be used to obtain high water flux. The rationale for the variation of the draw solution performance could be attributed to the aggregation of the nanoparticle at a higher concentration. According to Van't Hoff's equation [49], higher content of solute implies higher osmotic pressure. However, a contradicting result was obtained and this could be caused due to the aggregation of the nanoparticles at a higher amount of TiO<sub>2</sub> [50], [51]. This can be corrected by controlling the dispersion of the TiO<sub>2</sub> nanoparticle in the draw solution by applying longer ultrasonication. To prevent the aggregation of the nanoparticle at a higher amount, longer ultrasonication accompanied by pH adjustment were performed. The water flux result shown in Fig.6 was evaluated using the draw solution at a pH of 6. The value of the pH was adjusted to 4.5

using 0.01M HCl to investigate the performance of the draw solution for the higher content of TiO<sub>2</sub> NPs. Fig.8a and 8b demonstrates the effect of UV irradiation on water flux using 2g/L of TiO<sub>2</sub> NPs draw solution and sonicated for 25 min.

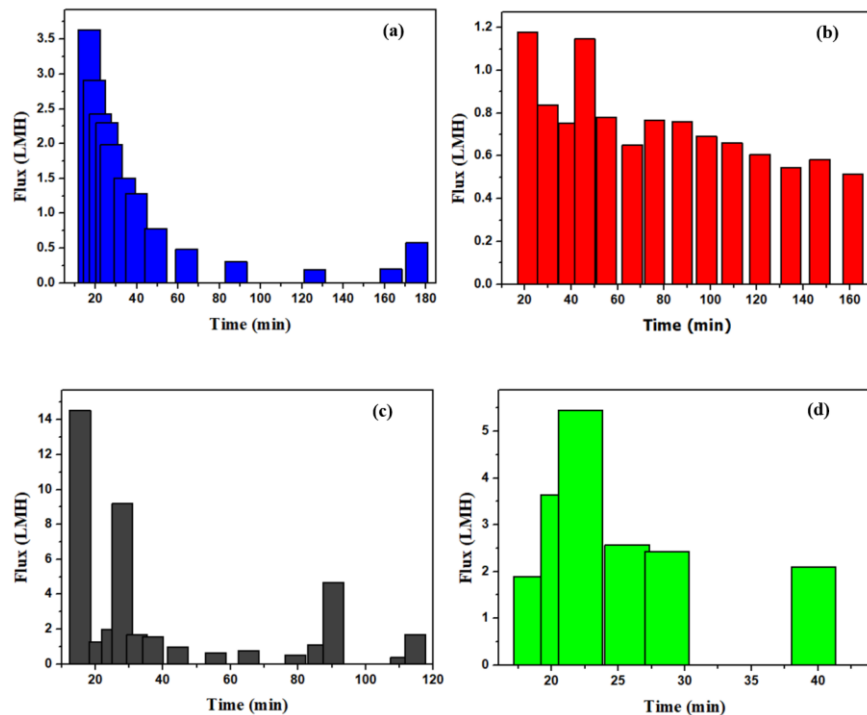


**Fig. 8.** Effect of ultrasonication on the performance of the draw solution using: (a) 2g/L, and (c) 5 g/L of of TiO<sub>2</sub> nanoparticle ultrasonicated for 25 min without UV treatment, (b) 2 g/L, and (d) 5 g/L of TiO<sub>2</sub> nanoparticle ultrasonicated for 25 min before 1 h UV treatment. All draw solutions were adjusted to a pH of 4.5.

It is apparent from Fig.8 that the draw solution sonicated at the aforementioned time it showed a positive result of water flux, while at the low period of sonication and at pH 6, almost no water flux was obtained. From Fig.8, it can be seen that the draw solution treated with UV (Fig. 8b) showed lower water flux than without treatment of UV (Fig. 8a). This result contradicts with the expected phenomenon where UV treatment increases the hydrophilicity of the stimuli-responsive materials like TiO<sub>2</sub> nanoparticle [52] which endows to enhance the driving force of the osmotic pressure, consequently lead to obtaining higher water flux. This behavior can be explained with the behavior of aggregation where UV treatment promotes aggregation of the nanoparticle and adversely affect the performance of the draw solution, which was also reported in [53].

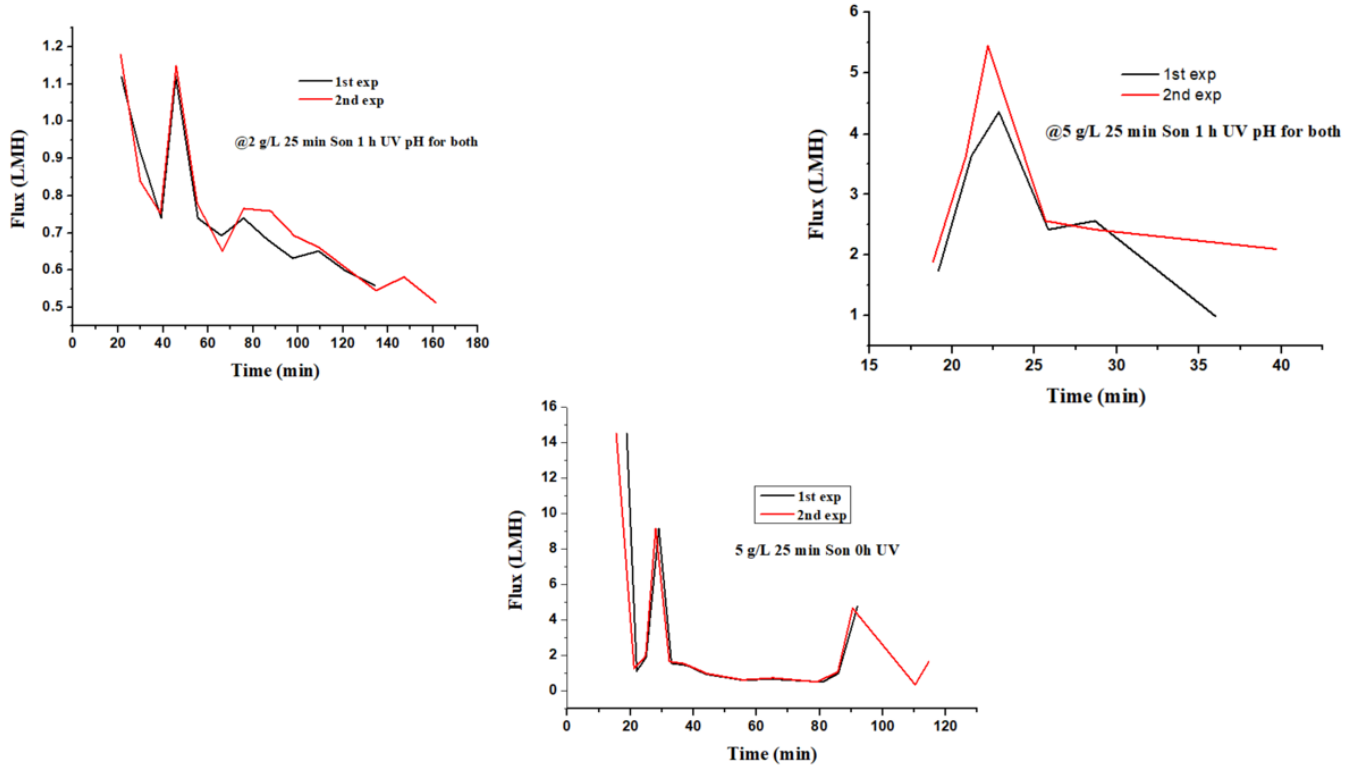


**Fig. 9.** Reproducibility result: Effect of ultrasonication on the performance of the draw solution

This unusual result was also confirmed by using 5g/L of TiO<sub>2</sub> NPs and the obtained results are shown in Fig.8c and 8d. To solve this problem, the draw solution was sonicated after UV treatment and the results revealed that a higher water flux can be obtained by sonicating before and after UV treatment for 25min. Moreover, the water flux performance of the draw solutions with lower TiO<sub>2</sub> nanoparticles concentrations without UV treatment was also evaluated. But, the results are not presented here since the values were insignificant.

#### 4.1.2 Effect of ultra-sonication

Fig.10 shows the effect of sonication before and after UV treatment and it is apparent that the ultrasonication helped to disperse the nanoparticle and leads to higher water flux. It can be seen that draw solution used for FO without sonication after UV offers lower water flux compared with draw solution sonicated before and after the UV treatment. This is due to the aid of the sonication that results to prevent the aggregation of the nanoparticle and promote the dispersion of the nanoparticle in the water which strength the driving force of the osmotic pressure. Fig.10.

demonstrates the effect of sonication of the draw solution on the performance of the water flux using 5g/L TiO<sub>2</sub> NPs. It was also observed that higher sonication does not imply higher water flux and this suggest that an optimal sonication could prevail.

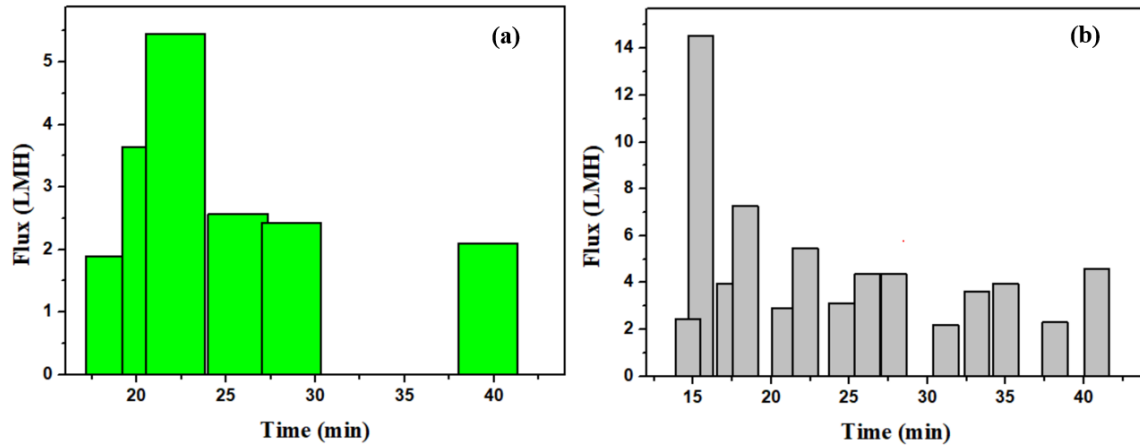


**Fig. 10.** Effect of sonication of the draw solution before and after UV treatment ( a) sonicated before UV (b) sonicated before and after UV for 25 min: 5g/L TiO<sub>2</sub> NPs at pH = 4.5

The reproducibility result of Fig.10 is shown below.

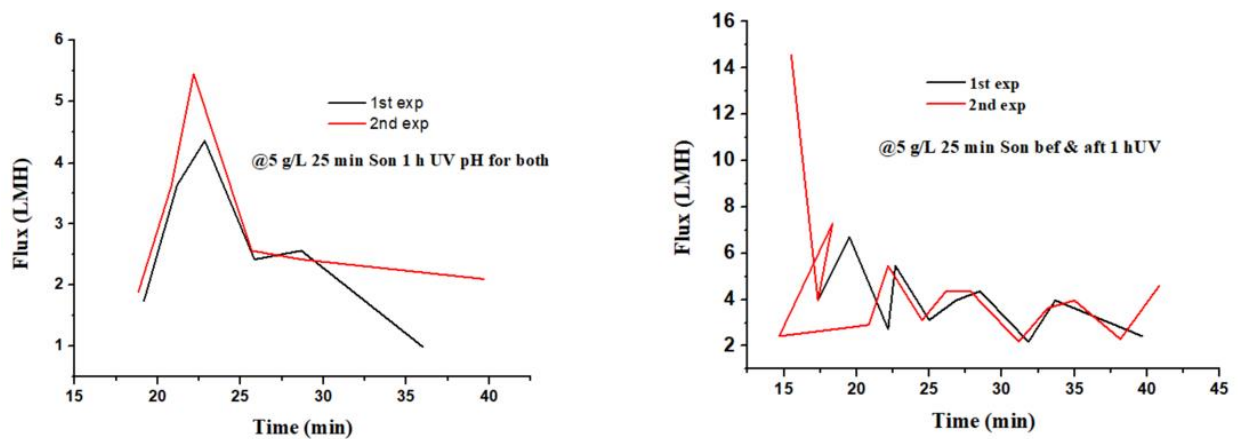


**Fig.11.** Reproducibility result: Effect of sonication of the draw solution before and after UV treatment

From Fig.12, It can conclude 25 min is the optimum sonication time. This is due to the fact that at higher sonication, hydrophilicity state of the nanoparticle shifts to hydrophobic state which is its original state [54]–[56].

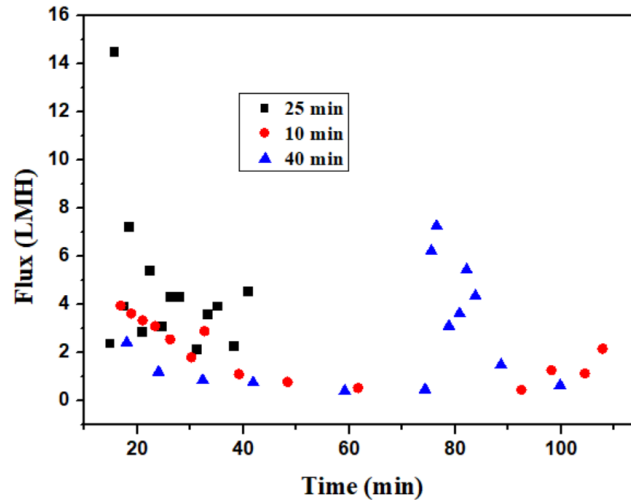


**Fig.12.** Effect of sonication time after 1 h UV treatment of the draw solution on the water flux in FO using 5g/L TiO<sub>2</sub> NPs sonicated for 25 min before 1 h UV treatment.

#### 4.1.3 Effect of concentration of TiO<sub>2</sub> nanoparticle

In the previous section, it was mentioned that the optimum sonication time and UV irradiation and the pH value. By using these optimized parameters, an FO experiment was conducted to find out the optimum concentration of TiO<sub>2</sub>. Fig.13 shows the effect of concentration of TiO<sub>2</sub> on the performance of the draw solution results showed that 20 g/L TiO<sub>2</sub> had significantly higher water flux than 5g/L. During the experiment, we have used 5, 20 g/L and 50 g/L TiO<sub>2</sub> and 20 g/L was obtained as optimum concentration. The data for 50 g/L TiO<sub>2</sub> is not presented here since the flux was very low. At higher concentration of TiO<sub>2</sub>, the viscosity of the draw solution become very high and hinder the diffusivity of water in the solution, consequently causes the osmotic pressure to be lower [57], [58]. The water fluxes of both concentrations (5 and 20 g/L) gradually reduced along with time, due to the reduced osmotic pressure across the membrane when the draw solution was diluted by the permeated water from feed solution (Fig.13).

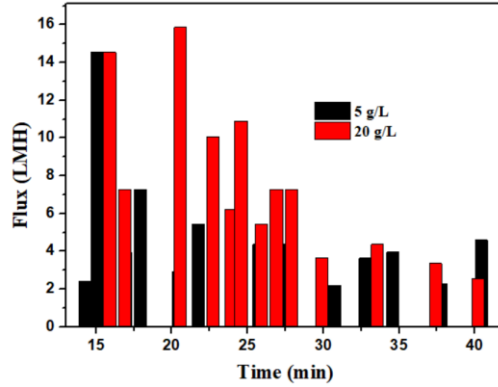


**Fig. 13.** Effect of concentration of TiO<sub>2</sub> on water flux: sonicated for 25min before and after 1 h UV irradiation at pH = 4.5.

The reproducibility of 20 g/L is depicted in the graph below.

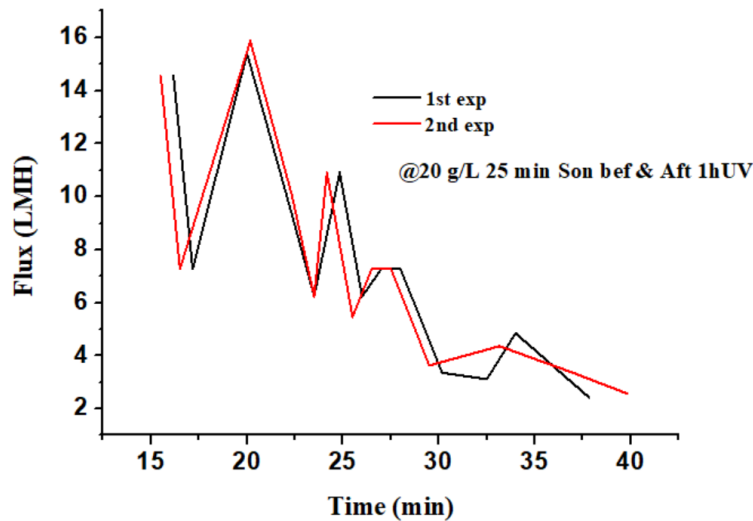


**Fig. 14.** Reproducibility result of 20 g/L

The TiO<sub>2</sub> NPs at 20 g/L can yield the highest water flux of 15.8 LMH without any functionalization or capping agent so that this FO water flux is quite promising (Fig.13). The TiO<sub>2</sub> NPs performance can be improved and exceed that of existing draw solutes with typical concentrations such as polyelectrolyte-functionalized magnetic nanoparticles [59], [60], [61], Polyelectrolytes [62], polymer hydrogels [63], Na<sup>+</sup>- functionalized carbon quantum dots [64].

#### 4.1.4. Effect of particle size of TiO<sub>2</sub>

The particle size of the draw solute has a significant effect on the performance of the draw solution. Fig 15 shows the effect of particle size of TiO<sub>2</sub> on the performance of the draw solution in FO experiment using DI water as feed solution. It was demonstrated that small particle size (5 nm) has higher water flux than the larger (25 nm). This is due to the fact that the smallest particles have a larger surface area to volume ratio, leading to a larger contact area and thus to a higher water flux [65].

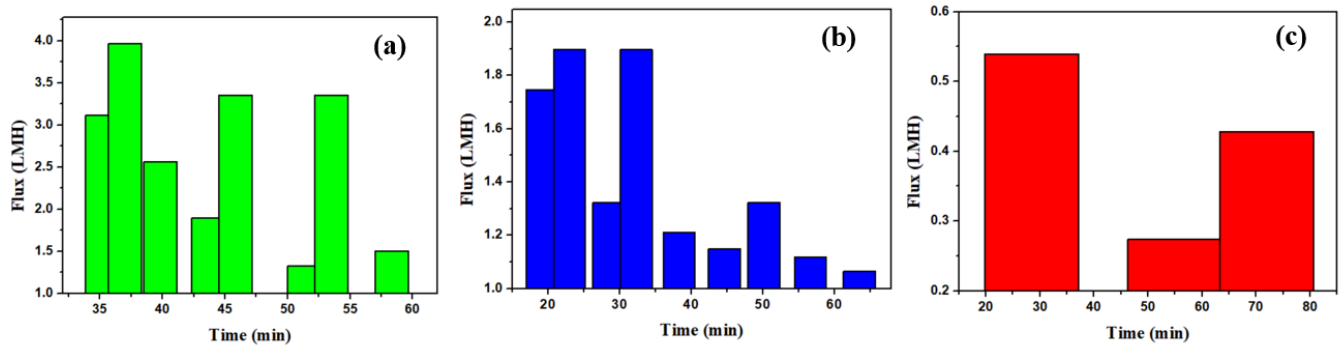


**Fig.15.** Effect of particle size of TiO<sub>2</sub> in draw solution performance in FO water flux: (a) P5, (b) P15, (c) P25 nm size.

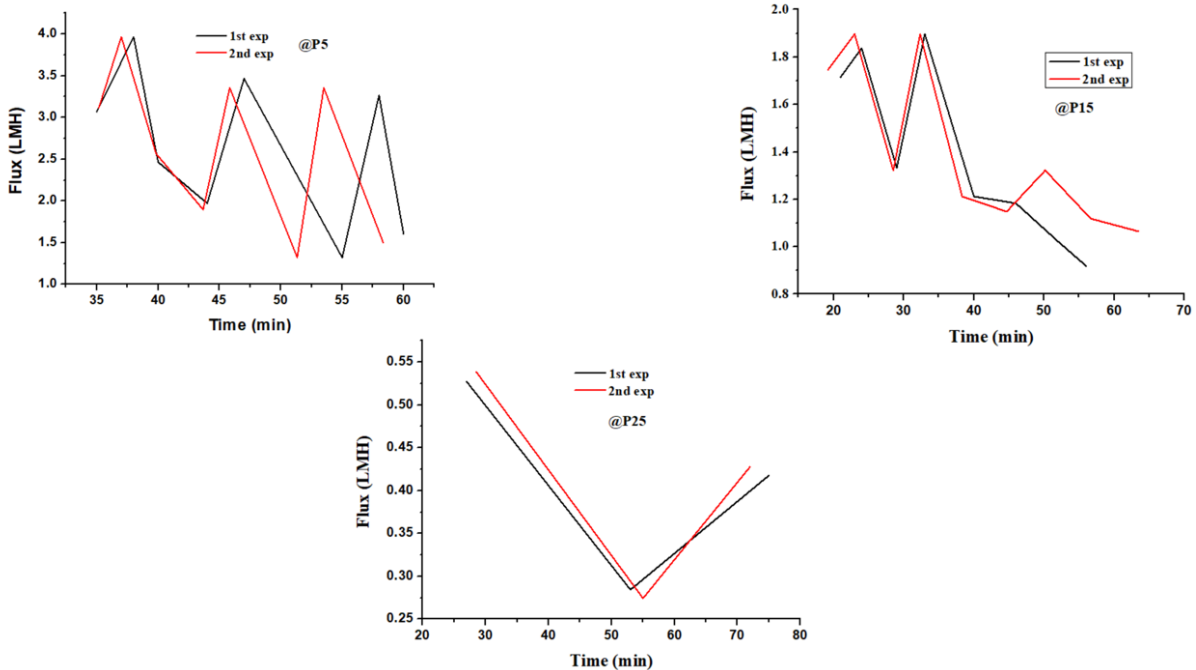


**Fig.16.** Reproducibility result: Effect of particle size of TiO<sub>2</sub> in draw solution performance in FO water flux

#### 4.1.5 Effect of membrane orientation

In addition to the draw solution, membrane orientation has also a significant effect on the performance of FO technology. During the experiment, two types of membrane orientation were used to investigate the effect on the water flux. Fig.17 shows the effect of two membrane orientation (PRO and FO) on the overall water flux in FO.

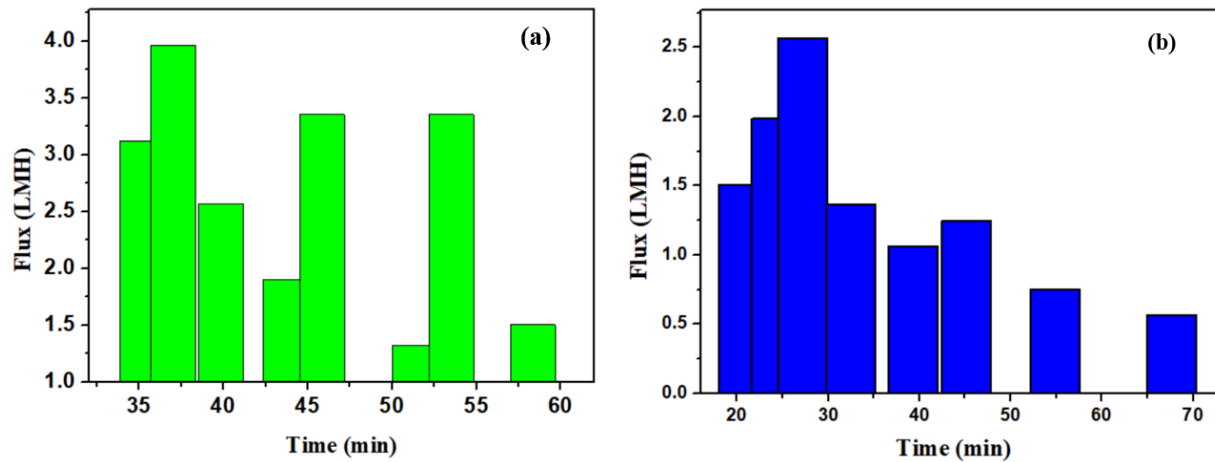


**Fig. 17.** Effect of membrane orientations on the FO water flux. (a) PRO mode, (b) FO mode

The optimized draw solution with 20 g/L TiO<sub>2</sub> NPs (P5) sonicated at 25 min before and after UV treatment without pH adjustment was used to evaluate the water flux performance of the two types of membrane orientation. Results disclosed that PRO mode (Fig. 17a) has a higher water flux than the FO mode (Fig. 17b). This is due to the effect of internal concentration polarization, which significantly reduces the available osmotic driving force [31].

#### 4.3 FO-Desalination

TiO<sub>2</sub> solution at 20 g/L without UV treatment was evaluated as FO draw solution using 500 ppm NaCl as a feed solution. Fig. 18 shows the weight of the feed solution measured in time. The weight of the feed solution linearly increased with time (Fig. 18) due to the transfer of water from the draw solution to the feed solution. This indicates that the osmotic pressure of feed solution was considerably higher than the draw solution osmotic pressure.

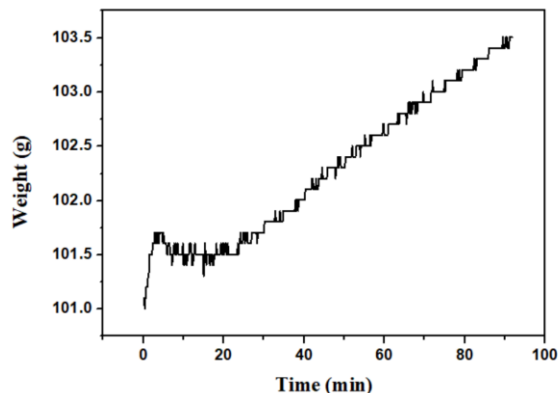


**Fig. 18.** Feed solution weight versus time profile recorded using 20 g/L TiO<sub>2</sub> draw solution without UV treatment sonicated for 25 minutes before FO experiment with 500 ppm NaCl feed solution.

In order to withdraw water from the 500 ppm NaCl solution the osmotic pressure of the draw solution should have higher osmotic pressure than the feed solution. To enhance its hydrophilicity and thereby to increase its osmotic pressure, the draw solution was treated with UV for 1 hour. Then after an FO experiment was conducted with 500 and 1000 ppm of NaCl feed solutions respectively. Based on the weight change of the TiO<sub>2</sub> solution during FO as shown in Fig. 19 (a) and (c), the fluxes were calculated. The FO was repeated 2 times and the water fluxes are summarized in Fig. 19 b and d. An initial FO water fluxes of 4.4 LMH was achieved with the 500 ppm NaCl feed solution. With 1000 ppm NaCl feed solution an initial flux of 1.2 LMH was obtained, but the rest of the evaluated fluxes were negative (Fig. 19 d).

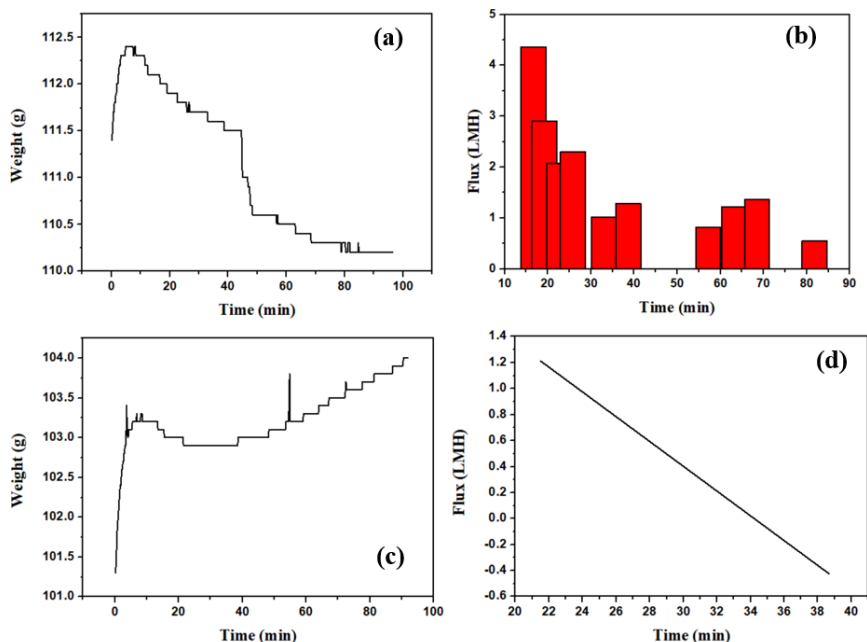


**Fig. 19.** Weight change of the feed solutions and evaluated Water fluxes based on the weight change of the feed solutions in 2h FO process by employing 20 g/L of TiO<sub>2</sub> concentration ultrasonicated for 25 minutes before and after UV treatment as draw solution. Weight change measured: (a) 500 ppm and (b) 1000 ppm NaCl solution feed solutions. Water fluxes calculated by using: (C) 500 ppm, and (d) 1000 ppm NaCl solutions as a feed solution.

To attract water completely from 1000 ppm and more, the draw solution was mixed with citric acid [66], but unfortunately, the addition of citric acid leads to sedimentation of TiO<sub>2</sub> nanoparticles, as a result, it only withdraw water from 100 ppm NaCl feed solution (Fig 20).

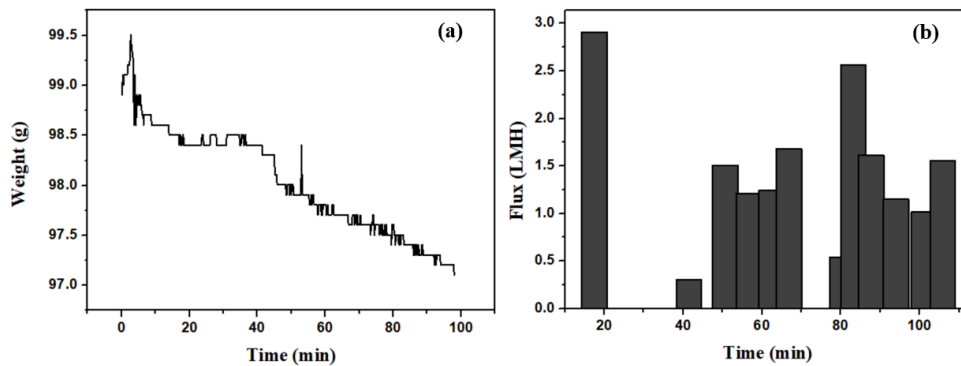


**Fig.20.** FO desalination with 20 g/L TiO<sub>2</sub> draw solution and 100 ppm NaCl feed solution: (a) weight versus time change of the feed solution, (b) water fluxes evaluated based on the weight change of the feed solution in time.

#### 4.2 Dynamic light scattering (DLS)

There was a significant effect of UV treatment on the TiO<sub>2</sub> nanoparticle size. As it is evident from Fig 21. The hydrodynamic diameter of the draw solution irradiated for 1 h in the UV oven was higher than the draw solution without UV treatment. But, after ultrasonication, the UV treated draw solution its hydrodynamic diameter becomes lower comparing to the pristine and the UV treated draw solution. The larger particle size leads to lower osmotic pressure since the interaction between the nanoparticles and the solvent (water) is weak [65].

Since osmotic pressure increases as the solubility of solute are higher and lower osmotic pressure means lower driving force or lower water flux. This result explains why lower flux was obtained after UV treatment as discussed in the above.

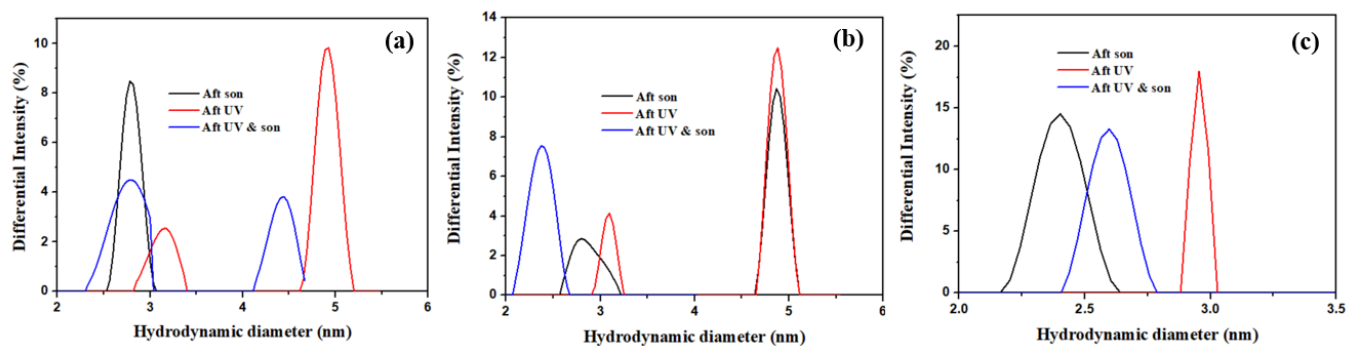


**Fig. 21.** Effect of UV treatment on the hydrodynamic diameter of the nanoparticles (in log to base 10): (a) = P5, (b) = P15, (c) = P25

**Table 3.** The measured Polydispersity Index (PDI) and Number of counts of the three types of TiO<sub>2</sub> NPS: P5, P15 and P25.

	P5		P15		P25	
	Polydispersity Index	Number of Counts (cps)	Polydispersity Index	Number of Counts (cps)	Polydispersity Index	Number of Counts (cps)
Aft Son	-0.632		-2.462	17421	0.352	15394
Aft UV	0.173	11164	0.67	14062	0.346	16328
Aft UV & Son	0.122	16746	0.133	11378	0.338	14054

The DLS measurement was conducted two times for each parameters to check the reproducibility of the results, but still negative values of PDI were observed for the P5 and P15.

### 4.3 FTIR

UV treatment of TiO<sub>2</sub> NPs for 4 h caused to moderately increase the deepness of the – OH peak whereas as the 1 h and 2 h UV treatment of TiO<sub>2</sub> NPs draw solution showed similar - OH stretching peak as shown in Fig 22. This deeper or strong OH stretching showed after 4 h UV irradiation is qualitatively an indicative of the presence of a moderately higher amount of adsorbed hydroxyl groups comparing to 1h and 2 h UV illumination. And a higher amount of adsorbed hydroxyl groups means more hydrophilic surface [52].

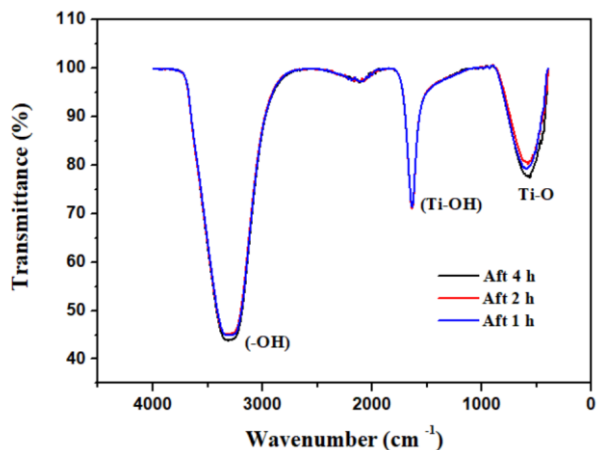


**Fig. 22.** FTIR result shows the effect of UV irradiation time on the chemical composition of TiO<sub>2</sub> NPs

#### 4.4 Recovery method

The TiO<sub>2</sub> NPs can be recovered easily via 2 main consecutive processes: (1) Dark storage, and (2) low-pressure driven-ultrafiltration processes as shown in Fig 23. The draw solution stored for 2 days in dark place showed less sedimentation of TiO<sub>2</sub> nanoparticles, but after 5 days storage, most of the TiO<sub>2</sub> NPs were sedimented or separated from the water (Fig. 23). Then after the remaining TiO<sub>2</sub> NPs can be separated easily via Low-pressure driven-ultrafiltration process followed by drying of the concentrated TiO<sub>2</sub> NPS. This intriguing advantage of the easy recovery of TiO<sub>2</sub> NPs meet the stringent criteria for an ideal draw solute.

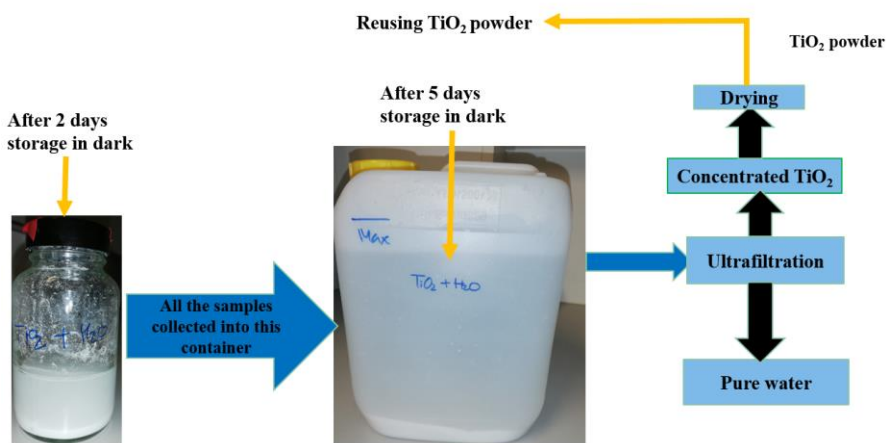


**Fig.23.** TiO<sub>2</sub> regeneration process from the diluted TiO<sub>2</sub> draw solution via two main consecutive processes: (1) dark storage, and (2) low-pressure Ultrafiltration processes

## 5 Conclusion

The study revealed that the flux generated by using pristine inorganic TiO<sub>2</sub> nanoparticles (P25) accompanied by low ultrasonication time ( $\leq 10$  min) were very low but after the colloidal stability of the draw solution was maintained via pH and longer ultrasonication, the performance of the draw solution dramatically increases. The performance of the draw solution was also further enhanced after UV treatment followed by ultrasonication. The highest flux generated with the optimized concentration of TiO<sub>2</sub> nanoparticles (20 g/L) and DI feed solution was 15.8 LMH. This flux is quite promising since it is obtained without using any functionalization groups. And it is believed that the water flux can be further increased via modification of the surface chemistry. Nanoparticles primary size and membrane orientations had a significant effect on the generated flux. P5 and PRO mode resulted in flux enhanced by more than 50% comparing to P25 and FO mode due to more contact area as a consequence of smaller particle size and higher driving force as a result of low concentration polarization respectively. Moreover, the draw solution was also characterized by DLS and FTIR to analyze the effect of UV irradiation on the particle size and also UV illumination time on hydrophilicity switch. And it was able to confirm that UV irradiation increases the hydrodynamic diameter of the nanoparticles unless it was not ultrasonicated after UV treatment. And the FTIR result revealed that longer UV irradiation (4h) of the TiO<sub>2</sub> nanoparticles slightly increases the strength of OH peak in relative to 1 and 2 h UV treatment which was an indication of the formation of the more hydrophilic surface. TiO<sub>2</sub> nanoparticles after being used in the FO process are readily regenerated via dark storage and low pressure driven-ultrafiltration. The dark storage facilitates the separation of most of the TiO<sub>2</sub> from the water and made the remaining much diluted draw solution to be separated with low energy consumption. Future studies will be focused on (1) the optimization of surface chemistry (2) the exploration of their performance in forward osmosis for brackish water desalination, and (3) the investigation of their sustainability in forward osmosis processes.

## References

- [1] Q. Ge, F. Fu, and T.-S. Chung, “Ferric and cobaltous hydroacid complexes for forward osmosis (FO) processes,” *Water Res.*, vol. 58, pp. 230–238, Jul. 2014.
- [2] “Water scarcity.” [Online]. Available: [https://www.sciencedaily.com/terms/water\\_scarcity.htm](https://www.sciencedaily.com/terms/water_scarcity.htm). [Accessed: 01-Mar-2019].
- [3] Y. Kang *et al.*, “Progress in Polymer Science Recent membrane development for pervaporation processes,” *Prog. Polym. Sci.*, vol. 57, pp. 1–31, 2016.
- [4] R. Semiat, “Critical Review Energy Issues in Desalination Processes,” vol. 42, no. 22, pp. 8193–8201, 2008.
- [5] N. Kress, “Desalination Technologies,” in *Marine Impacts of Seawater Desalination*, Elsevier, 2019, pp. 11–34.
- [6] A. D. Khawaji, I. K. Kutubkhanah, and J. Wie, “Advances in seawater desalination technologies,” vol. 221, pp. 47–69, 2008.
- [7] B. Mayor, “Growth patterns in mature desalination technologies and analogies with the energy field,” *Desalination*, vol. 457, no. January, pp. 75–84, 2019.
- [8] M. B. El-arnaouty, A. M. A. Ghaffar, M. Eid, M. E. Aboufotouh, N. H. Taher, and E. Soliman, “Journal of Radiation Research and Applied Sciences Nano-modification of polyamide thin film composite reverse osmosis membranes by radiation grafting,” *J. Radiat. Res. Appl. Sci.*, vol. 11, no. 3, pp. 204–216, 2018.
- [9] A. Al-Karaghoul and L. L. Kazmerski, “Energy consumption and water production cost of conventional and renewable-energy-powered desalination processes,” *Renew. Sustain. Energy Rev.*, vol. 24, pp. 343–356, Aug. 2013.
- [10] A. Al-Karaghoul and L. L. Kazmerski, “Energy consumption and water production cost of conventional and renewable-energy-powered desalination processes,” *Renew. Sustain.*

*Energy Rev.*, vol. 24, pp. 343–356, 2013.

- [11] A. S. Stillwell and M. E. Webber, “Predicting the specific energy consumption of reverse osmosis desalination,” *Water (Switzerland)*, vol. 8, no. 12, pp. 1–18, 2016.
- [12] Y. Ghalavand, M. S. Hatamipour, and A. Rahimi, “A review on energy consumption of desalination processes,” *Desalin. Water Treat.*, vol. 54, no. 6, pp. 1526–1541, 2015.
- [13] J. A. Carta, J. González, P. Cabrera, and V. J. Subiela, “Preliminary experimental analysis of a small-scale prototype SWRO desalination plant, designed for continuous adjustment of its energy consumption to the widely varying power generated by a stand-alone wind turbine,” *Appl. Energy*, vol. 137, pp. 222–239, 2015.
- [14] J. M. Veza, B. Penate, and F. Castellano, “Electrodialysis desalination designed for off-grid wind energy,” *Desalination*, vol. 160, no. 3, pp. 211–221, 2004.
- [15] E. Jones, M. Qadir, M. T. H. van Vliet, V. Smakhtin, and S. Kang, “The state of desalination and brine production: A global outlook,” *Sci. Total Environ.*, vol. 657, pp. 1343–1356, Mar. 2019.
- [16] D. Wu, A. Gao, H. Zhao, and X. Feng, “Pervaporative desalination of high-salinity water,” *Chem. Eng. Res. Des.*, vol. 136, pp. 154–164, 2018.
- [17] J. R. McCutcheon, R. L. McGinnis, and M. Elimelech, “A novel ammonia-carbon dioxide forward (direct) osmosis desalination process,” *Desalination*, vol. 174, no. 1, pp. 1–11, 2005.
- [18] H. Jaramillo, S. Lin, D. L. Shaffer, M. Elimelech, and J. R. Werber, “Forward osmosis: Where are we now?,” *Desalination*, vol. 356, pp. 271–284, 2014.
- [19] H. Luo *et al.*, “Journal of Water Process Engineering A review on the recovery methods of draw solutes in forward osmosis,” *J. Water Process Eng.*, vol. 4, pp. 212–223, 2014.
- [20] Y. Cai and X. M. Hu, “A critical review on draw solutes development for forward osmosis,” *DES*, vol. 391, pp. 16–29, 2016.
- [21] J. R. McCutcheon, R. L. McGinnis, and M. Elimelech, “Desalination by ammonia-carbon

- dioxide forward osmosis: Influence of draw and feed solution concentrations on process performance,” *J. Memb. Sci.*, vol. 278, no. 1–2, pp. 114–123, 2006.
- [22] R. L. McGinnis, J. R. McCutcheon, and M. Elimelech, “A novel ammonia-carbon dioxide osmotic heat engine for power generation,” *J. Memb. Sci.*, vol. 305, no. 1–2, pp. 13–19, 2007.
- [23] P. Liu *et al.*, “Water flux behavior of blended solutions of ammonium bicarbonate mixed with eight salts respectively as draw solutions in forward osmosis,” *Desalination*, vol. 353, pp. 39–47, 2014.
- [24] M. I. T. Opencourseware, “Review of Water Resources and Desalination Technologies,” 2009.
- [25] F. S. Pinto and R. C. Marques, “Desalination projects economic feasibility : A standardization of cost determinants,” *Renew. Sustain. Energy Rev.*, vol. 78, no. February, pp. 904–915, 2017.
- [26] A. A. Abufayed, M. K. A. Elghuelb, and M. Rashedb, “Desalination : a viable supplemental source of water for the arid states of North Afkica,” vol. 152, 2002.
- [27] T. Chung, S. Zhang, K. Yu, J. Su, and M. Ming, “Forward osmosis processes : Yesterday , today and tomorrow,” *DES*, vol. 287, pp. 78–81, 2012.
- [28] S. Zhao, L. Zou, C. Y. Tang, and D. Mulcahy, “Recent developments in forward osmosis: Opportunities and challenges,” *J. Memb. Sci.*, vol. 396, pp. 1–21, 2012.
- [29] B. D. Coday *et al.*, “The sweet spot of forward osmosis : Treatment of produced water , drilling wastewater , and other complex and dif fi cult liquid streams,” *DES*, vol. 333, no. 1, pp. 23–35, 2014.
- [30] Q. Ge, M. Ling, and T. Chung, “Draw solutions for forward osmosis processes : Developments , challenges , and prospects for the future,” *J. Memb. Sci.*, vol. 442, pp. 225–237, 2013.
- [31] J. R. Mccutcheon and M. Elimelech, “Influence of concentrative and dilutive internal

- concentration polarization on flux behavior in forward osmosis,” vol. 284, pp. 237–247, 2006.
- [32] D. J. Johnson, W. A. Suwaileh, A. W. Mohammed, and N. Hilal, “Osmotic ’ s potential : An overview of draw solutes for forward osmosis G R A P H I C A L A B S T R A C T,” *Desalination*, vol. 434, no. August 2017, pp. 100–120, 2018.
- [33] H. Bai, Z. Liu, and D. D. Sun, “Highly water soluble and recovered dextran coated Fe<sub>3</sub>O<sub>4</sub> magnetic nanoparticles for brackish water desalination,” *Sep. Purif. Technol.*, vol. 81, no. 3, pp. 392–399, Oct. 2011.
- [34] Q. Ge, J. Su, T.-S. Chung, and G. Amy, “Hydrophilic Superparamagnetic Nanoparticles: Synthesis, Characterization, and Performance in Forward Osmosis Processes,” *Ind. Eng. Chem. Res.*, vol. 50, no. 1, pp. 382–388, Jan. 2011.
- [35] J. Kim, J. Kim, J. Lim, and S. Hong, “Evaluation of ethanol as draw solute for forward osmosis (FO) process of highly saline (waste)water,” *Desalination*, vol. 456, pp. 23–31, Apr. 2019.
- [36] A. Shakeri, M. T. Nakhjiri, H. Salehi, F. Ghorbani, and N. Khankeshipour, “Preparation of polymer-carbon nanotubes composite hydrogel and its application as forward osmosis draw agent,” *J. Water Process Eng.*, vol. 24, pp. 42–48, Aug. 2018.
- [37] A. Rahardianto, W. Y. Shih, R. W. Lee, and Y. Cohen, “Diagnostic characterization of gypsum scale formation and control in RO membrane desalination of brackish water,” *J. Memb. Sci.*, vol. 279, no. 1–2, pp. 655–668, 2006.
- [38] M. L. Stone, C. Rae, F. F. Stewart, and A. D. Wilson, “Switchable polarity solvents as draw solutes for forward osmosis,” *Desalination*, vol. 312, pp. 124–129, 2013.
- [39] T. Alejo, M. Arruebo, V. Carcelen, V. M. Monsalvo, and V. Sebastian, “Advances in draw solutes for forward osmosis: Hybrid organic-inorganic nanoparticles and conventional solutes,” *Chem. Eng. J.*, vol. 309, pp. 738–752, 2017.
- [40] D. Li and H. Wang, “Smart draw agents for emerging forward osmosis application,” *J. Mater. Chem. A*, vol. 1, no. 45, pp. 14049–14060, 2013.

- [41] E. Tian *et al.*, “A study of poly (sodium 4-styrenesulfonate) as draw solute in forward osmosis,” *Desalination*, vol. 360, pp. 130–137, 2015.
- [42] D. Zhao, P. Wang, Q. Zhao, N. Chen, and X. Lu, “Thermoresponsive copolymer-based draw solution for seawater desalination in a combined process of forward osmosis and membrane distillation,” *Desalination*, vol. 348, pp. 26–32, 2014.
- [43] H. T. Nguyen, S. S. Chen, N. C. Nguyen, H. H. Ngo, W. Guo, and C. W. Li, “Exploring an innovative surfactant and phosphate-based draw solution for forward osmosis desalination,” *J. Memb. Sci.*, vol. 489, pp. 212–219, 2015.
- [44] G. T. Gray, J. R. Mccutcheon, and M. Elimelech, “Internal concentration polarization in forward osmosis " role of membrane orientation,” 2006.
- [45] M. Miyauchi, A. Nakajima, T. Watanabe, and K. Hashimoto, “Photocatalysis and Photoinduced Hydrophilicity of Various Metal Oxide Thin Films,” no. 24, pp. 2812–2816, 2002.
- [46] R. Sun, A. Nakajima, A. Fujishima, and T. Watanabe, “Photoinduced Surface Wettability Conversion of ZnO and TiO<sub>2</sub> Thin Films,” no. 4, pp. 1984–1990, 2001.
- [47] K. Liu, M. Cao, A. Fujishima, and L. Jiang, “Bio-Inspired Titanium Dioxide Materials with Special Wettability and Their Applications,” 2014.
- [48] M. Miyauchi, N. Kieda, S. Hishita, and T. Mitsuhashi, “Reversible wettability control of TiO<sub>2</sub> surface by light irradiation,” vol. 511, pp. 401–407, 2002.
- [49] “Vant hoff’s eqqn.pdf.” .
- [50] M. H. El-rafie, T. I. Shaheen, A. A. Mohamed, and A. Hebeish, “Bio-synthesis and applications of silver nanoparticles onto cotton fabrics,” *Carbohydr. Polym.*, vol. 90, no. 2, pp. 915–920, 2012.
- [51] A. Sotto *et al.*, “Journal of Colloid and Interface Science Effect of nanoparticle aggregation at low concentrations of TiO<sub>2</sub> on the hydrophilicity , morphology , and fouling resistance of PES – TiO<sub>2</sub> membranes,” *J. Colloid Interface Sci.*, vol. 363, no. 2,

- pp. 540–550, 2011.
- [52] R. Wang, N. Sakai, A. Fujishima, and T. Watanabe, “Studies of Surface Wettability Conversion on TiO<sub>2</sub> Single-Crystal Surfaces,” pp. 2188–2194, 1999.
- [53] J. Sun, L. Guo, H. Zhang, and L. Zhao, “UV Irradiation Induced Transformation of TiO<sub>2</sub> Nanoparticles in Water: Aggregation and Photoreactivity,” 2014.
- [54] R. Wang, N. Sakai, A. Fujishima, and T. Watanabe, “Studies of Surface Wettability Conversion on TiO<sub>2</sub> Single-Crystal Surfaces,” pp. 2188–2194, 1999.
- [55] A. Weissler, “Formation of Hydrogen Peroxide by Ultrasonic Waves : Free Radicals,” vol. 93, no. 3, pp. 3–7, 1959.
- [56] N. Sakai, R. Wang, A. Fujishima, and T. Watanabe, “Effect of Ultrasonic Treatment on Highly Hydrophilic TiO<sub>2</sub> Surfaces,” vol. 7463, no. 98, pp. 5918–5920, 1998.
- [57] C. Suh and S. Lee, “Modeling reverse draw solute flux in forward osmosis with external concentration polarization in both sides of the draw and feed solution,” *J. Memb. Sci.*, vol. 427, pp. 365–374, 2013.
- [58] S. Zhao and L. Zou, “Relating solution physicochemical properties to internal concentration polarization in forward osmosis,” *J. Memb. Sci.*, vol. 379, no. 1–2, pp. 459–467, 2011.
- [59] M. M. Ling, K. Y. Wang, and T. Chung, “Highly Water-Soluble Magnetic Nanoparticles as Novel Draw Solutes in Forward Osmosis for Water Reuse,” no. Iii, pp. 5869–5876, 2010.
- [60] Z. Y. Liu, H. W. Bai, and D. D. Sun, “Nanoparticles as Draw Solution for Forward Osmosis Processes,” pp. 115–128, 2008.
- [61] Q. Zhao, N. Chen, D. Zhao, and X. Lu, “Thermoresponsive Magnetic Nanoparticles for Seawater Desalination,” 2013.
- [62] Q. Ge, J. Su, G. L. Amy, and T. S. Chung, “Exploration of polyelectrolytes as draw solutes in forward osmosis processes,” *Water Res.*, vol. 46, no. 4, pp. 1318–1326, 2012.

- [63] D. Li, X. Zhang, J. Yao, P. Simon, and H. Wang, “ChemComm Stimuli-responsive polymer hydrogels as a new class of draw agent for forward osmosis desalination w,” pp. 1710–1712, 2011.
- [64] V. A. Online, C. X. Guo, P. Wang, and X. Lu, “Na<sup>+</sup>-functionalized carbon quantum dots : a new draw solute in forward osmosis for seawater desalination †,” pp. 7318–7321, 2014.
- [65] A. Razmjou, G. P. Simon, and H. Wang, “Effect of particle size on the performance of forward osmosis desalination by stimuli-responsive polymer hydrogels as a draw agent,” *Chem. Eng. J.*, vol. 215–216, pp. 913–920, 2013.
- [66] E. Cheraghipour, S. Javadpour, and A. R. Mehdizadeh, “Citrate capped superparamagnetic iron oxide nanoparticles used for hyperthermia therapy,” vol. 2012, no. December, pp. 715–719, 2012.